Nonperturbative effects in gluon radiation and photoproduction of quark pairs

Boris Kopeliovich
Max-Planck Institut für Kernphysik, Postfach 103980, 69029 Heidelberg, Germany
and Joint Institute for Nuclear Research, Dubna, 141980 Moscow Region, Russia

Andreas Schäfer
Institut für Theoretische Physik, Universität Regensburg, 93040 Regensburg, Germany

Alexander Tarasov
Max-Planck Institut für Kernphysik, Postfach 103980, 69029 Heidelberg, Germany,
Joint Institute for Nuclear Research, Dubna, 141980 Moscow Region, Russia,
and Institut für Theoretische Physik, Universitat Regensburg, 93040 Regensburg, Germany
(Received 9 August 1999; published 9 August 2000)

We introduce a nonperturbative interaction for light-cone fluctuations containing quarks and gluons. The $\bar{q}q$ interaction squeezes the transverse size of these fluctuations in the photon and one does not need to simulate this effect via effective quark masses. The strength of this interaction is fixed by data. Data on diffractive dissociation of hadrons and photons show that the nonperturbative interaction of gluons is much stronger. We fix the parameters for the nonperturbative quark-gluon interaction by data for diffractive dissociation to large masses (triple-Pomeron regime). This allows us to predict nuclear shadowing for gluons which turns out to be not as strong as perturbative QCD predicts. We expect a delayed onset of gluon shadowing at $x \leqslant 10^{-2}$ shadowing of quarks. Gluon shadowing turns out to be nearly scale invariant up to virtualities $Q^2 \sim 4$ GeV^2 due to the presence of a semihard scale characterizing the strong nonperturbative interaction of gluons. We use the same concept to improve our description of gluon bremsstrahlung which is related to the distribution function for a quark-gluon fluctuation and the interaction cross section of a $\bar{q}qG$ fluctuation with a nucleon. We expect the nonperturbative interaction to suppress dramatically the gluon radiation at small transverse momenta compared to perturbative calculations.

PACS number(s): 12.38.Lg, 12.38.Bx, 13.60.Hb

I. INTRODUCTION

The light-cone representation introduced in [1] is nowadays a popular and powerful tool to study the dynamics of photo-induced (real and virtual) reactions. The central concept of this approach is the non-normalized distribution amplitude of $\bar{q}q$ fluctuations of the photon in the mixed $(\vec{\rho}, \alpha)$ representation, where $\vec{\rho}$ is the transverse $\bar{q}q$ separation and α is the fraction of the light-cone momentum of the photon carried by the quark (antiquark). For transversely and longitudinally polarized photons it reads [1,2]

$$\Psi_{qq}^{T,L}(\vec{\rho},\alpha)=\frac{\sqrt{\alpha_{em}}}{2\pi}\bar{\chi}\hat{O}^{T,L}\chi K_0(\epsilon\rho). \tag{1}$$

Here χ and $\bar{\chi}$ are the spinors of the quark and antiquark respectively. $K_0(\epsilon\rho)$ is the modified Bessel function, where

$$\epsilon^2=\alpha(1-\alpha)Q^2+m_q^2. \tag{2}$$

This is a generalization of [1,2] to the case of virtual photons [3,4].

The operators $\hat{O}^{T,L}$ have the form

$$\hat{O}^T=m_q\,\vec{\sigma}\cdot\vec{e}+i(1-2\alpha)(\vec{\sigma}\cdot\vec{n})(\vec{e}\cdot\vec{\nabla}_\rho)+(\vec{\sigma}\times\vec{e})\cdot\vec{\nabla}_\rho, \tag{3}$$

$$\hat{O}^L=2Q\alpha(1-\alpha)\vec{\sigma}\cdot\vec{n}, \tag{4}$$

where the dimension-two operator $\vec{\nabla}_\rho$ acts on the transverse coordinate $\vec{\rho}$; $\vec{n}=\vec{p}/p$ is a unit vector parallel to the photon momentum; $\vec{e}$ is the polarization vector of the photon.

The advantage of the light-cone approach is the factorized form of the interaction cross section which is given by the sum of the cross sections for different fluctuations weighted by the probabilities of these Fock states [5,3,6]. The flavor independent color-dipole cross section σ_{qq}^- first introduced in [5] as dependent only on transverse $\bar{q}q$ separation ρ. It vanishes quadratically at $\rho\to 0$ due to color screening,

$$\sigma_{qq}^-(\rho,s)\big|_{\rho\to 0}=C(\rho,s)\rho^2, \tag{5}$$

where $C(\rho,s)$ is a smooth function of separation and energy. In fact, $C(\rho,s)$ also depends on relative sharing by the $\bar{q}$ and q of the total light cone momentum. We drop this dependence in what follows unless it is important (e.g. for diffractive gluon radiation). It was first evaluated assuming no energy dependence in perturbative QCD (PQCD) [5,7] and phenomenologically [8] at medium large energies and ρ's and turned out to be $C\approx 3$. There are several models for the function $C(\rho,s)$ (e.g., in [9–11]), unfortunately neither seems to be reliable. In this paper we concentrate on the principal problems of how to include nonperturbative effects

and do not try to optimize the form of the cross section. For practical applications it can be corrected as soon as a more reliable model for $C(\rho,s)$ is available. We modify one of the models mentioned above [10] which keeps the calculations simple to make it more realistic and use it throughout this paper.

The distribution amplitudes (1) control the mean transverse $\bar{q}q$ separation in a virtual photon:

$$\langle \rho^2 \rangle \sim \frac{1}{\alpha(1-\alpha)Q^2+m_q^2}. \tag{6}$$

Thus, even a highly virtual photon can create a large size $\bar{q}q$ fluctuation with large probability provided that α (or $1-\alpha$) is very small, $\alpha Q^2 \sim m_q^2$. This observation is central to the aligned jet model [2]. At small Q^2 soft hadronic fluctuations become dominant at any α. In this case the perturbative distribution functions (1) which are based on several assumptions including asymptotic freedom, are irrelevant. One should expect that nonperturbative interactions modify (squeeze) the distribution of transverse separations of the $\bar{q}q$ pair. In Sec. II A we introduce a nonperturbative interaction between the quark and antiquark into the Schrödinger type equation for the Green function of the $\bar{q}q$ pair [12–14]. The shape of the real part of this potential is adjusted to reproduce the light-cone wave function of the ρ-meson. We derive new light-cone distribution functions for the interacting $\bar{q}q$ fluctuations of a photon, which coincide with the known perturbative ones in the limit of vanishing interaction. The strength of the nonperturbative interaction can be fixed by comparison with data sensitive to the transverse size of the fluctuations. The observables we have chosen in Sec. II B are the total photoabsorption cross sections on protons and nuclei and the cross section for diffractive dissociation of a photon into a $\bar{q}q$ pair.

For gluon bremsstrahlung we expect the transverse separation in a quark-gluon fluctuation to be of the order of the typical color correlation length ~ 0.3 fm obtained by several QCD analyses [15–17]. This corresponds to the radius of a constituent quark in many effective models. To the extend that the typical $q-G$ separation is smaller than the $\bar{q}q$ one we expect gluon radiation to be suppressed. This results in particular in a suppression of diffractive gluon radiation, i.e., of the triple-Pomeron coupling, which is seen indeed in the data.

In Sec. III A we assume a similar shape for the quark-gluon potential as for the $\bar{q}q$ one, but with different parameters. A new light-cone distribution function for a quark-gluon fluctuation of a quark is derived, which correctly reproduces the known limit of perturbative QCD.

Comparison with data on diffractive excitations with large mass fixes the strength of the nonperturbative interaction of gluons. An intuitive physical picture of diffraction, as well as a simple calculation of the cross sections of different diffractive reactions is presented in Appendix A. A more formal treatment of the same diffractive reactions via calculation of Feynman diagrams is described in Appendix B.

A crude estimate of the interaction parameters is given in Sec. III A 1 within the additive quark model (AQM). For this purpose the cross section of diffractive gluon radiation by a quark, $qN \to q\,GN$, is calculated in Appendices A 2 and B 1, based on general properties of diffraction (Appendix A 1) and the direct calculation of Feynman diagrams.

Quite a substantial deviation from the results for the AQM is found in Sec. III A 2 and Appendix C where the diffractive excitation of a nucleon via gluon radiation, $NN \to XN$ is calculated. The high precision of the data for this reaction allows to fix the strength of the nonperturbative interaction of gluons rather precisely.

The cross sections of diffractive gluon radiation by mesons and photons are calculated in Appendixes A 3 and B 2. In Sec. III A 3 we compare the values of the triple-Pomeron couplings (calculated in Appendix C) for diffractive dissociation of a photon and different hadrons and find a violation of Regge factorization by about a factor of two.

Our results for the cross section of diffractive dissociation $\gamma^* N \to q\bar{q}GN$ in the limit of vanishing nonperturbative interaction can be compared with previous perturbative calculations [18,19]. In this limit we are in agreement with [19], but disagree with [18].[1] The source of error in [18] is the application of Eq. (A6) to an exclusive channel and a renormalization recipe based on a probabilistic treatment of diffraction.

Diffractive radiation of photons is considered in Appendices A 4 and B 3. It is shown that no radiation occurs without transverse momentum transfer to the quark (in contrast to gluon radiation). Therefore, the cross section for diffractive production of Drell-Yan pairs is suppressed compared to the expectation of [20] which is also based on an improper application of Eq. (A6) to an exclusive channel.

Section III B is devoted to nuclear shadowing for the gluon distribution function at small x. Calculations for many hard reactions on nuclei [deep inelastic scattering (DIS), high p_T jets, heavy flavor production, etc.] desperately need the gluon distribution function for nuclei which is expected to be shadowed at small x. Many approaches [21–31] to predict nuclear shadowing for gluons can be found in the literature (see recent review [32]). Our approach is based on Gribov's theory of inelastic shadowing [33] and is close to that in [30,31] which utilizes the results [34,35] for the gluonic component of the diffractive structure function assuming factorization and using available data. Instead, we fix the parameters of the nonperturbative interaction using data on diffraction of protons and real photons. Besides, we achieved substantial progress in understanding the evolution of diffractively produced intermediate states in nuclear matter.

Nuclear suppression of the gluon density which looks like a result of gluon fusion $GG \to G$ in the infinite momentum frame of the nucleus, should be interpreted as usual nuclear shadowing for the total interaction cross section of fluctua-

[1] In spite of the claim in [19] that their result coincides with that of [18], they are quite different. We are thankful to Mark Wüsthoff for discussion of this controversy.

tions containing a gluon if seen in the rest frame of the nucleus. We perform calculations for longitudinally polarized photons which are known to be a good probe for the gluon distribution function. Although the physics of nuclear shadowing and diffraction are closely related, even a good knowledge of single diffractive cross section and mass distributions is not sufficient to predict nuclear shadowing completely, but only the lowest order shadowing correction. A technique for inclusion of the multiple scattering corrections was developed in [12,13] which includes evolution of the intermediate states propagating through the nucleus. These corrections are especially important for gluon shadowing which does not saturate even at very small x in contrast to shadowing of quarks. In Sec. III B 1 we find quite a steep x-dependence of gluon shadowing at $Q^2 \geqslant 4$ GeV^2 which is rather weak compared to what have been estimated in [30,31]. Shadowing starts at smaller values of $x<0.01$ compared to the shadowing of quarks. Such a delayed onset of gluon shadowing is a result of enlarged mass of the fluctuations containing gluons.

As soon as our approach incorporates the nonperturbative effects we are in position to calculate shadowing for soft gluons as well. This is done in Sec. III B 2 using two methods. In hadronic basis one can relate the shadowing term in the total hadron-nucleus cross section to the known diffractive dissociation cross section. This also give the scale for the effective absorption cross section. A better way is to apply the Green function approach which includes the nonperturbative gluon interaction fixed by comparison with data for diffraction. With both methods we have arrived at a similar shadowing, but the Green function approach leads to a delayed onset of shadowing starting at $x<0.01$. We conclude that gluon shadowing is nearly scale independent up to $Q^2 \sim 4$ GeV^2.

The nonperturbative interaction of the radiated gluons especially affects their transverse momentum distribution. One can expect a substantial suppression of radiation with small k_T related to large transverse separations in quark-gluon fluctuations of the projectile quark. Indeed, in Sec. III C we have found suppression by almost two orders of magnitude for radiation at $k_T=0$ compared to the perturbative QCD predictions. The difference remains quite large up to a few GeV of momentum transfer. Especially strong nonperturbative effects we expect for the k_T distribution of gluon bremsstrahlung by a quark propagating through a nucleus. Instead of a sharp peak at $k_T=0$ predicted by PQCD [36] now we expect a minimum.

II. VIRTUAL PHOTOPRODUCTION OF QUARK PAIRS

A. Green function of an interacting quark-antiquark pair

Propagation within a medium of an interacting $\bar{q}q$ pair which has been produced with initial separation $\rho=0$ from a virtual photon at a point with longitudinal coordinate z_1 and developed a separation $\vec{\rho}$ at the point z_2 (see Fig. 1) can be described by a light-cone Green function $G^{-}_{qq}(z_1,\vec{\rho}_1=0;z_2,\vec{\rho}_2=\vec{\rho})$. The evolution equation for this Green function was studied in [12–14],[2]

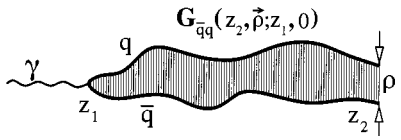

FIG. 1. Illustration for the Green function $G^{-}_{qq}(z_1,\vec{\rho}_1=0;z_2,\vec{\rho}_2=\vec{\rho})$ for an interacting $\bar{q}q$ fluctuation of a photon, as defined by Eq. (7).

$$i\frac{d}{dz_2}G^{-}_{qq}(z_1,\vec{\rho}_1;z_2,\vec{\rho}_2) = \left[\frac{\epsilon^2-\Delta_\rho}{2\,p\,\alpha(1-\alpha)}+V^{-}_{qq}(z_2,\vec{\rho},\alpha)\right]G^{-}_{qq}(z_1,\vec{\rho}_1;z_2,\vec{\rho}_2). \tag{7}$$

The first term on the right-hand side (RHS) is analogous to the kinetic term in a Schrödinger equation. It takes care of the phase shift for the propagating $\bar{q}q$ pair. Indeed, the relevant phase factor is given by $\exp[i\int_{z_1}^{z_2}dz\,q_L(z)]$, with the relative longitudinal momentum transfer q_L. The latter is defined by

$$q_L(z)=\frac{M^2(z)+Q^2}{2p}=\frac{\epsilon^2+k_T^2}{2p\alpha(1-\alpha)}. \tag{8}$$

Here p is the photon momentum; M is the effective mass of the $\bar{q}q$ pair (which varies with z) and Q^2 is the photon virtuality. It depends on the transverse momentum k_T of the quark (antiquark) which is replaced by the Laplacian, $k_T^2 \Rightarrow -\Delta_\rho$, in the coordinate representation (7).

The imaginary part of the potential $V^{-}_{qq}(z_2,\vec{\rho},\alpha)$ is responsible for absorption in the medium which is supposed to be cold nuclear matter:

$$\mathrm{Im}\,V^{-}_{qq}(z_2,\vec{\rho},\alpha)=-\frac{\sigma^{-}_{qq}(\rho)}{2}\rho_A(z_2). \tag{9}$$

Here $\rho_A(z)$ is the nuclear density and we omit the dependence on the nuclear impact parameter. $\sigma^{-}_{qq}(\rho,s)$ is the total interaction cross section of a colorless $\bar{q}q$ pair with a nucleon [5] introduced in Eq. (5). Equation (7) with the imaginary potential (9) was used in [12] to calculate nuclear shadowing

[2]Our Green function is related to that in [12] by

$$G^{-}_{qq}(z_1,\vec{\rho}_1=0;z_2,\vec{\rho}_2=\vec{\rho}) = \exp[-i\epsilon^2(z_2-z_1)/2p\alpha(1-\alpha)] \times W(z_1,\rho_1=0;z_2,\rho_2=\rho).$$

in deep-inelastic scattering. In other applications the quarks were treated as free, what is justified only in the domain of validity of perturbative QCD.

Our objective here is to include explicitly the nonperturbative interaction between the quarks in Eq. (7). We are going to rely on a nonrelativistic potential, which, however, should be modified to be a function of the light-cone variables $\vec{\rho}$ and α. This general problem is, however, not yet solved. Nevertheless, we try to model the real part of the potential based on its general properties. Particularly, the $\overline{q}q$ pair is supposed to have bound states which are vector mesons.

It is assumed usually that the wave function of a vector meson in the ground state depends on ρ and α according to

$$\Psi_V(\vec{\rho},\alpha)=f(\alpha)\exp\left[-\frac{1}{2}a^2(\alpha)\vec{\rho}^2\right]. \tag{10}$$

In order for this to be a solution of Eq. (7) the real part of the potential should be

$$\mathrm{Re}\, V_{\overline{q}q}(z_2,\vec{\rho},\alpha)=\frac{a^4(\alpha)\vec{\rho}^2}{2p\alpha(1-\alpha)}. \tag{11}$$

Unfortunately, no reliable way to fix the form of $a(\alpha)$ is known. A parametrization popular in the literature is $a(\alpha)=2a\sqrt{\alpha(1-\alpha)}$, which results from attempts to construct a relativistic approach to the problem of a $\overline{q}q$ bound state (see [37] and references therein). In this case, however, the mean $\overline{q}q$ separation $\rho\propto 1/\sqrt{\alpha(1-\alpha)}$ increases unrestrictedly towards the endpoints $\alpha=0,1$. Such a behavior contradicts the concept of confinement and should be corrected. The simplest way to do so is to add a constant term to $a(\alpha)$ [the real form of $a(\alpha)$ may be quite different, but so far data allow only for a simple two parameter fit],

$$a^2(\alpha)=a_0^2+4a_1^2\alpha(1-\alpha). \tag{12}$$

One can roughly evaluate a_0 by demanding that even at $\alpha=0,1$ the transverse $\overline{q}q$ separation does not exceed the confinement radius,

$$a_0\sim R_c^{-1}\approx\Lambda_{QCD}, \tag{13}$$

i.e., $a_0\approx 200$ MeV. Comparison with data (see below) leads to a somewhat smaller value.

In what follows we study the consequences of the interaction between q and $\overline{q}$ in the form (11),(12) for the quark wave function of the photon, and we discuss several observables.

Let us denote the Green function of a $\overline{q}q$ pair propagating in vacuum ($\mathrm{Im}\, V=0$) as $G_{\overline{q}q}(z_1,\vec{\rho}_1;z_2,\vec{\rho}_2)$. The solution of Eq. (7) has the form [38]

$$G_{\overline{q}q}(z_1,\vec{\rho}_1;z_2,\vec{\rho}_2)=\frac{a^2(\alpha)}{2\pi i\sin(\omega\,\Delta z)}\exp\left\{\frac{ia^2(\alpha)}{2\sin(\omega\,\Delta z)}\times[(\rho_1^2+\rho_2^2)\cos(\omega\Delta z)-2\vec{\rho}_1\cdot\vec{\rho}_2]-\frac{i\epsilon^2\Delta z}{2p\alpha(1-\alpha)}\right\}, \tag{14}$$

where $\Delta z=z_2-z_1$ and

$$\omega=\omega(\alpha)=\frac{a^2(\alpha)}{p\alpha(1-\alpha)}. \tag{15}$$

The normalization factor here is fixed by the condition $G_{\overline{q}q}(z_1,\vec{\rho}_1;z_2,\vec{\rho}_2)|_{z_2=z_1}=\delta^2(\vec{\rho}_1-\vec{\rho}_2)$.

Now we are in the position to calculate the distribution function of a $\overline{q}q$ fluctuation of a photon including the interaction. It is given by the integral of the Green function over the longitudinal coordinate z_1 of the point at which the photon forms the $\overline{q}q$ pair (see Fig. 1),

$$\Psi_{\overline{q}q}^{T,L}(\vec{\rho},\alpha)=\frac{i\,Z_q\sqrt{\alpha_{em}}}{4\pi p\alpha(1-\alpha)}\int_{-\infty}^{z_2}dz_1(\overline{\chi}\hat{O}^{T,L}\chi)\times G_{\overline{q}q}(z_1,\vec{\rho}_1;z_2,\vec{\rho}_2)|_{\rho_1=0;\vec{\rho}_2=\vec{\rho}}. \tag{16}$$

The operators $\hat{O}^{T,L}$ are defined in Eqs. (4)–(6). Here they act on the coordinate $\vec{\rho}_1$.

If we write the transverse part as

$$\overline{\chi}\hat{O}^T\chi=A+\vec{B}\cdot\vec{\nabla}_{\rho_1}, \tag{17}$$

then the distribution functions read

$$\Psi_{\overline{q}q}^{T}(\vec{\rho},\alpha)=Z_q\sqrt{\alpha_{em}}\,[A\,\Phi_0(\epsilon,\rho,\lambda)+\vec{B}\,\vec{\Phi}_1(\epsilon,\rho,\lambda)], \tag{18}$$

$$\Psi_{\overline{q}q}^{L}(\vec{\rho},\alpha)=2\,Z_q\sqrt{\alpha_{em}}\,Q\alpha(1-\alpha)\,\overline{\chi}\vec{\sigma}\cdot\vec{n}\chi\Phi_0(\epsilon,\rho,\lambda), \tag{19}$$

where

$$\lambda=\lambda(\alpha)=\frac{2\,a^2(\alpha)}{\epsilon^2}. \tag{20}$$

The functions $\Phi_{0,1}$ in Eqs. (18),(19) are defined as

$$\Phi_0(\epsilon,\rho,\lambda)=\frac{1}{4\pi}\int_0^\infty dt\,\frac{\lambda}{\mathrm{sh}(\lambda t)}\exp\left[-\frac{\lambda\epsilon^2\rho^2}{4}\mathrm{cth}(\lambda t)-t\right], \tag{21}$$

$$\vec{\Phi}_1(\epsilon,\rho,\lambda)=\frac{\epsilon^2\vec{\rho}}{8\pi}\int_0^\infty dt\left[\frac{\lambda}{\mathrm{sh}(\lambda t)}\right]^2\exp\left[-\frac{\lambda\epsilon^2\rho^2}{4}\mathrm{cth}(\lambda t)-t\right]. \tag{22}$$

Note that the $q-\bar{q}$ interaction emerges in Eqs. (18),(19) through the parameter λ defined in Eq. (20). In the limit $\lambda \to 0$ (i.e. $Q^2 \to 0$, α is fixed, $\alpha \neq 0$ or 1) we get the well known perturbative expressions (1) for the distribution functions,

$$\Phi_0(\epsilon,\rho,\lambda)|_{\lambda=0} \Rightarrow \frac{1}{2\pi} K_0(\epsilon\rho), \tag{23}$$

$$\vec{\Phi}_1(\epsilon,\rho,\lambda)|_{\lambda=0} \Rightarrow \frac{\epsilon\vec{\rho}}{2\pi\rho} K_1(\epsilon\rho) = -\frac{1}{2\pi}\vec{\nabla} K_0(\epsilon\rho). \tag{24}$$

In contrast to these relations, in the general case, i.e., for $\lambda \neq 0$,

$$\vec{\Phi}_1(\epsilon,\rho,\lambda) \neq -\vec{\nabla}\Phi_0(\epsilon,\rho,\lambda). \tag{25}$$

In the strong interaction limit $\lambda \gg m_q$ [or if both (Q^2, $m_q \to 0$)] which is appropriate particularly for real photons and massless quarks, the functions $\Phi_{0,1}$ acquire again simple analytical forms,

$$\Phi_0(\epsilon,\rho,\lambda)|_{\lambda\to\infty} \Rightarrow \frac{1}{4\pi} K_0\left[\frac{1}{2}a^2(\alpha)\rho^2\right], \tag{26}$$

$$\vec{\Phi}_1(\epsilon,\rho,\lambda)|_{\lambda\to\infty} \Rightarrow \frac{\vec{\rho}}{2\pi\rho^2}\exp\left[-\frac{1}{2}a^2(\alpha)\rho^2\right]. \tag{27}$$

The interaction confines even massless quarks within a finite range of ρ.

B. Absorption cross section for virtual photons

For highly virtual photons, $Q^2 \gg a^2(\alpha)$, according to Eq. (20) $\lambda \to 0$ and the effects related to the nonperturbative $\bar{q}q$ interaction should be gone. Although for very asymmetric configurations, $\alpha(1-\alpha) \ll 1$, see Eq. (2) the transverse $\bar{q}q$ separation increases and one may expect the nonperturbative interaction to be at work, it does not happen if the dipole cross section is independent of ρ at large ρ.

Thus, our equations show a smooth transition between the formalism of perturbative QCD valid at high Q^2 and our model for low Q^2 where nonperturbative effects are important.

The absorption cross sections for transversely (T) and longitudinally (L) polarized virtual photons , including the nonperturbative effects, read

$$\sigma_{tot}^T = 2N_c \sum_F Z_q^2 \alpha_{em} \int_0^1 d\alpha \int d^2\rho \sigma_{qq}^-(\rho,s) \times \{m_q^2 \Phi_0^2(\epsilon,\rho,\lambda) + [\alpha^2 + (1-\alpha)^2]\,|\vec{\Phi}_1(\epsilon,\rho,\lambda)|^2\}, \tag{28}$$

$$\sigma_{tot}^L = 8Q^2 N_c \sum_F Z_q^2 \alpha_{em} \int_0^1 d\alpha\,\alpha \times (1-\alpha) \int d^2\rho \sigma_{qq}^-(\rho,s)\Phi_0^2(\epsilon,\rho,\lambda). \tag{29}$$

Here N_c is the number of colors, and the contributions of different flavors F are summed up.

According to Eq. (5) the dipole cross section vanishes $\sigma_{qq}^-(\rho,s) \propto \rho^2$ at small $\rho \ll 1$ fm. Such a behavior approximately describes, e.g., the observed hierarchy of hadronic cross sections as functions of the mean hadronic radii [8]. We expect, however, that the dipole cross section flattens off at larger separations $\rho > 1$ fm. Therefore, the approximation $\sigma_{qq}^-(\rho) \propto \rho^2$ is quite crude for the large separations typical for soft reactions. Even the simple two-gluon approximation [39,40] provides only a logarithmic growth at large ρ [5], and confinement implies a cross section which becomes constant at large ρ. Besides, the energy dependence of the dipole cross section is stronger at small ρ than at large ρ [41]. We use hereafter a parametrization similar to one suggested in [10]:

$$\sigma_{qq}^-(\rho,s) = \sigma_0(s)\left[1 - \exp\left(-\frac{\rho^2}{\rho_0^2(s)}\right)\right], \tag{30}$$

where $\rho_0(s) = 0.88$ fm $(s_0/s)^{0.14}$ and $s_0 = 1000$ GeV^2. In contrast to [10] all values depend on energy (as it is supposed to be) rather than on x and we introduce an energy dependent parameter $\sigma_0(s)$,

$$\sigma_0(s) = \sigma_{tot}^{\pi p}(s)\left(1 + \frac{3\rho_0^2(s)}{8\langle r_{ch}^2\rangle_\pi}\right), \tag{31}$$

otherwise one fails to reproduce hadronic cross sections. Here $\langle r_{ch}^2\rangle_\pi = 0.44 \pm 0.01$ fm^2 [42] is the mean square of the pion charge radius. Cross section (30) averaged with the pion wave function squared automatically reproduces the pion-proton cross section. We use the results of the fit [43] for the Pomeron part of the cross section,

$$\sigma_{tot}^{\pi p}(s) = 23.6\,(s/s_0)^{0.08} \text{ mb}, \tag{32}$$

where $s_0 = 1000$ GeV^2. We fixed the parameters comparing data with the proton structure function calculated using Eqs. (28),(29) and the cross section (30). Agreement is reasonably good up to $Q^2 \sim 20$ GeV^2 sufficient for our purposes.

To fix from data the parameters $a_{0,1}$ of the potential we concentrate on real photoabsorption which is most sensitive to nonperturbative corrections. The photoabsorption cross section with free quark fluctuations in the photon diverges logarithmically at $m_q \to 0$,

$$\sigma_{tot}^T \approx \sigma_0 \ln\left(\frac{1}{m_q\rho_0}\right). \tag{33}$$

Inclusion of interaction between the quarks in the photon makes the photoabsorption cross section finite at $m_q \to 0$.

$$\sigma_{tot}^{T}=\sigma_0\frac{\alpha_{em}N_c}{12\pi}\sum_F Z_q^2[\phi(x_1)-\phi(x_2)], \tag{34}$$

where

$$x_1=\frac{1+a_0^2\rho_0^2}{a_1^2\rho_0^2};\quad x_2=\frac{a_0^2}{a_1^2}, \tag{35}$$

and

$$\phi(x)=4\ln\left(\frac{x}{4}\right)-2x+(4+x)\sqrt{1+x}\ \ln\left(\frac{\sqrt{1+x}+1}{\sqrt{1+x}-1}\right). \tag{36}$$

In this case the cross section of photoabsorption is independent of the quark mass in the limit $m_q/a_{0,1}\ll 1$.

We adjust the values of a_0 and a_1 to the value of the photoabsorption cross section $\sigma_{tot}^{\gamma p}=160\ \mu$b at $\sqrt{s}=200$ GeV [44,45]. Equation (34) alone does not allow to fix the two parameters a_0 and a_1 completely, but it provides a relation between them. We found a simple way to parametrize this ambiguity. If we choose

$$a_0^2=v^{1.15}(112\ \ \mathrm{MeV})^2$$

$$a_1^2=(1-v)^{1.15}(165\ \ \mathrm{MeV})^2, \tag{37}$$

the total photoabsorption cross section, turns out to be constant (within 1%) if v varies between 0 and 1. This covers all possible choices for a_0 and a_1.

In order to fix v in Eq. (37) one needs additional experimental information. We have tried a comparison with the following data.

(i) The cross section of forward diffraction dissociation $\gamma N\to\overline{q}qN$ (the PPR graph in the triple-Reggeon phenomenology [46]),

$$\left.\frac{d\sigma(\gamma N\to\overline{q}qN)}{dt}\right|_{t=0}=\frac{1}{16\pi}\int d\alpha\, d^2\rho\,|\Psi_{\overline{q}q}(\alpha,\rho)|^2\sigma^2(\rho). \tag{38}$$

(ii) The total photoabsorption cross sections for nuclei (high-energy limit),

$$\sigma_{tot}^{\gamma A}=2\int d^2b\int d\alpha\, d^2\rho\,|\Psi_{\overline{q}q}(\alpha,\rho)|^2\times\left\{1-\exp\left[\frac{1}{2}\sigma(\rho)T(b)\right]\right\}, \tag{39}$$

where

$$T(b)=\int_{-\infty}^{\infty}dz\,\rho_A(b,z) \tag{40}$$

is the nuclear thickness function and the nuclear density $\rho_A(b,z)$ depends on impact parameter b and longitudinal coordinate z. This expression can be used for virtual photons as well with a proper discrimination between transverse and longitudinal photons.

A calculation of the observables (i) and (ii) shows, however, a surprising stability of the results against variation of v in Eq. (37): the cross sections change only within $\sim 1\%$ if v varies between 0 and 1. Thus, we were unable to constrain the parameters a_0 and a_1 any further.

We have also calculated the effective interaction cross section of a $\overline{q}q$ pair with a nucleon,

$$\sigma_{eff}^{\overline{q}qN}=\frac{\int d\alpha\, d^2\rho\,|\Psi_{\overline{q}q}(\alpha,\rho)|^2\sigma^2(\rho,s)}{\int d\alpha\, d^2\rho\,|\Psi_{\overline{q}q}(\alpha,\rho)|^2\sigma(\rho,s)}\equiv\frac{\langle\sigma^2\rangle}{\langle\sigma\rangle}, \tag{41}$$

which is usually used to characterize shadowing for the interaction of the $\overline{q}q$ fluctuation of a real photon with a nucleus (e.g., see in [30,31]). We got at $\sigma_{eff}^{\overline{q}qN}=30$ mb at $\sqrt{s}=200$ GeV. This well corresponds to the pion-nucleon cross section (32) $\sigma_{tot}^{\pi p}=31.7$ mb at this energy. This result might be treated as success of the vector dominance model (VDM). On the other hand, a calculation [47] using VDM and $\sigma_{tot}^{\pi p}\approx 25$ mb instead of $\sigma_{tot}^{\rho p}$ at lower energy for photoproduction of ρ-mesons off nuclei is in good agreement with recent HERMES measurements [48,49].

However, a word of caution is in order. The nucleus to nucleon ratio of total photoabsorption cross sections in the approximation of frozen fluctuations (reasonably good at very small x) reads [5,30,31]

$$\frac{\sigma_{tot}^{\gamma^* A}}{A\,\sigma_{tot}^{\gamma^* N}}=\frac{2}{\langle\sigma\rangle}\int d^2b\left\langle 1-\exp\left[-\frac{\sigma}{2}T(b)\right]\right\rangle, \tag{42}$$

Expanding the exponential up to the next term after the double scattering one (1/4) σ_{eff} one gets (1/24) $\langle\sigma^3\rangle/\langle\sigma\rangle$. This is 1.5 times larger than (1/24) $\sigma_{eff}^2/\langle\sigma\rangle$ if to use the dipole approximation $\sigma\propto\rho^2$ and a Gaussian distribution over ρ for color triplet $(\overline{q}-q)$ or color octet $(G-\overline{q}q)$ dipoles.

III. GLUON BREMSSTRAHLUNG

A. Radiation of interacting gluons

In processes with radiation of gluons, like

$$q+N\to q+G+X \tag{43}$$

$$\gamma^*+N\to q+\overline{q}+G+X, \tag{44}$$

the interaction between the radiated gluon and the parent quark traveling in nearly the same direction may be important and significantly change the radiation cross section and the transverse momentum distribution compared to perturbative QCD calculations [50,36,51].

We describe the differential cross section of gluon radiation in a quark-nucleon collision in the factorized light-cone approach [36]

$$\frac{d^3\sigma(q\to qG)}{d(\ln\alpha)\,d^2k_T}=\frac{1}{(2\pi)^2}\int d^2r_1\,d^2r_2 \times\exp[i\vec{k}_T(\vec{r}_1-\vec{r}_2)]\,\Psi^*_{Gq}(\alpha,\vec{r}_1)\,\Psi_{Gq}(\alpha,\vec{r}_2) \times\sigma_G(\vec{r}_1,\vec{r}_2,\alpha), \tag{45}$$

where

$$\sigma_G(\vec{r}_1,\vec{r}_2,\alpha)=\frac{1}{2}\{\sigma_{G\bar{q}q}(\vec{r}_1,\vec{r}_1-\alpha r_2) +\sigma_{G\bar{q}q}(\vec{r}_2,\vec{r}_2-\alpha r_1) -\sigma_{\bar{q}q}[\alpha(\vec{r}_1-\vec{r}_2)]-\sigma_{GG}(\vec{r}_1-\vec{r}_2)\}. \tag{46}$$

Hereafter we assume all cross sections to depend on energy, but do not show it explicitly for the sake of brevity (unless it is important).

The cross section of a colorless $G\bar{q}q$ system with a nucleon $\sigma_{G\bar{q}q}(\vec{r}_1,\vec{r}_2)$ is expressed in terms of the usual $\bar{q}q$ dipole cross sections,

$$\sigma_{G\bar{q}q}(\vec{r}_1,\vec{r}_2)=\frac{9}{8}\{\sigma_{\bar{q}q}(r_1)+\sigma_{\bar{q}q}(r_2)\}-\frac{1}{8}\sigma_{\bar{q}q}(\vec{r}_1-\vec{r}_2) \tag{47}$$

$\vec{r}_1$ and $\vec{r}_2$ are the transverse separations gluon-quark and gluon-antiquark, respectively. In Eq. (46) $\sigma_{GG}(r)=\frac{9}{4}\sigma_{\bar{q}q}(r)$ is the total cross section of a colorless GG dipole with a nucleon.

The cross sections of reactions (43),(44) integrated over k_T have the simple form

$$\frac{d\sigma(q\to qG)}{d(\ln\alpha)}=\frac{1}{(2\pi)^2}\int d^2r\,|\Psi_{Gq}(\alpha,\vec{r})|^2\sigma_{G\bar{q}q}[\vec{r},(1-\alpha)\vec{r}], \tag{48}$$

$$\left.\frac{d\sigma(\gamma^*\to q\bar{q}G)}{d(\ln\alpha_G)}\right|_{\alpha_G\ll 1} =\int_0^1 d\alpha_q\int d^2R\;\;|\Psi^{\gamma^*}_{qq}(R,\alpha_q)|^2 \times\int d^2r\{|\Psi_{\bar{q}G}(\vec{R}+\vec{r},\alpha_G)|^2\sigma^N_{GG}(\vec{R}+\vec{r}) +|\Psi_{qG}(\vec{r},\alpha_G)|^2\sigma_{GG}(r)-\mathrm{Re}\,\Psi^*_{qG}(\vec{r},\alpha_G)\,\Psi_{\bar{q}G} \times(\vec{R}+\vec{r},\alpha_G)\,[\sigma_{GG}(\vec{R}+\vec{r})+\sigma_{GG}(r)-\sigma_{GG}(R)]\}. \tag{49}$$

Here α_G is the fraction of the quark momentum carried by the gluon; $\vec{R}$ and $\vec{r}$ are the quark-antiquark and quark-gluon transverse separations respectively. The three terms in the curly brackets in Eq. (49) correspond to the radiation of the gluon by the quark, by the antiquark, and to their interference, respectively.

The key ingredient of Eqs. (45), (48), and (49) is the distribution function $\Psi_{Gq}(\alpha,\vec{r})$ of the quark-gluon fluctuation, where α is the fraction of the light-cone momentum of the parent quark carried by the gluon, and $\vec{r}$ is the transverse quark-gluon separation. This function has a form [36,52,53] similar to Eq. (1),

$$\Psi^T_{Gq}(\alpha,\vec{r})|_{free}=\frac{1}{\pi}\sqrt{\frac{\alpha_s}{3}}\chi_f\hat{\Gamma}^{T,L}\chi_i K_0(\tau r_T), \tag{50}$$

where the operator $\hat{\Gamma}^T$ is defined in [36],

$$\hat{\Gamma}^T=im_q\alpha^2\vec{e^*}\cdot(\vec{n}\times\vec{\sigma})+\alpha\,\vec{e^*}\cdot(\vec{\sigma}\times\vec{\nabla})-i(2-\alpha)\,\vec{e^*}\cdot\vec{\nabla}. \tag{51}$$

We treat the gluons as massless since we incorporate the nonperturbative interaction explicitly and do not need to introduce any effective mass.

The factor τ differs from ϵ as defined in Eq. (2):

$$\tau^2=\alpha^2m_q^2. \tag{52}$$

In the general case the distribution function including the interaction between the quark and gluon can be found via the Green function $G_{qG}(z_1,\vec{\rho}_1;z_2,\vec{\rho}_2)$ for the propagation of a quark-gluon pair, in analogy to Eq. (16),

$$\Psi_{qG}(\vec{\rho},\alpha)=\frac{i\sqrt{\alpha_s/3}}{2\pi p\alpha(1-\alpha)}\int_{-\infty}^{z_2}dz_1\,(\overline{\chi\hat{\Gamma}}^T\chi) \times G_{qG}(z_1,\vec{\rho}_1;z_2,\vec{\rho}_2)\Big|_{\rho_1=0;\,\vec{\rho}_2=\vec{\rho}}. \tag{53}$$

Let us add a few comments as to why this direct analogy holds. Equation (46) might give the impression that we would have to implement the interaction between all three partons: the gluon, the quark and the antiquark. Checking the way in which this equation was derived, one realizes, however, that this is not the case. We studied gluon bremsstrahlung from a single quark and then expressed the radiation amplitude as a difference between the inelastic amplitudes for a qG system and an individual $\bar{q}$. This is how $\sigma_{G\bar{q}q}$ has to be interpreted and this is why one should only take the $q-G$ nonperturbative interaction into account.

The evolution equation for the Green function of an interacting qG pair originating from the parent quark at the point with longitudinal coordinate z_1 with initial transverse separation $\rho_1=0$ looks similar to Eq. (7) with the replacement $\epsilon\Rightarrow\tau$ and $V_{\bar{q}q}(z_2,\vec{\rho},\alpha)\Rightarrow V_{qG}(z_2,\vec{\rho},\alpha)$. We parameterize the quark-gluon potential in the same way as in Eq. (11) for quark-antiquark,

$$\mathrm{Re}\,V_{qG}(z_2,\vec{\rho},\alpha)=\frac{b^4(\alpha)\vec{\rho}^2}{2p\alpha(1-\alpha)}, \tag{54}$$

where $b^2(\alpha)=b_0^2+4\,b_1^2\,\alpha(1-\alpha)$.

The solution of the evolution equation for the quark-gluon Green function in absence of absorption ($\mathrm{Im}\, V_{qG}=0$) looks the same as Eq. (14) with replacement $a(\alpha)\Rightarrow b(\alpha)$.

The following transformations go along with Eqs. (16)–(27). The vertex function in Eq. (53) is represented as

$$\overline{\chi\hat{\Gamma}}^T\chi = D + \vec{E}\cdot\vec{\nabla}_{\rho_1}, \tag{55}$$

then the result of integration in Eq. (53) is

$$\Psi_{qG}(\vec{\rho},\alpha) = 2\sqrt{\left(\frac{\alpha_s}{3}\right)}\,[D\,\Phi_0(\tau,\rho,\lambda)+\vec{E}\cdot\vec{\Phi}_1(\tau,\rho,\lambda)]. \tag{56}$$

The functions $\Phi_0(\tau,\rho,\lambda)$ and $\vec{\Phi}_1(\tau,\rho,\lambda)$ are defined in Eqs. (21),(22). However, λ is now defined by

$$\lambda = \frac{2\,b^2(\alpha)}{\tau^2}. \tag{57}$$

One might argue that the quark-gluon potential we need (and which we shortly shall constrain by comparison with experimental data) could simply be obtained by adding two quark-quark potentials with an appropriate color factor. Such a procedure could, however, lead to a completely wrong results as we want to illustrate by the following example.

Motivated by perturbative QCD one might expect that the gluon-gluon and quark-quark potentials differ simply by a factor 9/4 (the ratio of the Casimir factors). However, this relation is affected by nontrivial properties of the QCD vacuum which makes the interaction of gluons much stronger [54,17]. The octet string tension κ_8 is related to α_P', the slope of the Pomeron trajectory in the same way as the color triplet string tension relates to the slope of the meson Regge trajectories [55],

$$\kappa_8 = \frac{1}{2\pi\alpha_P'} \approx 4 \ \ \mathrm{GeV/fm}. \tag{58}$$

Here $\alpha_P'=0.25\ \mathrm{GeV}^{-2}$. Thus, the value of κ_8 is in fact four times larger than the well known $\overline{qq}$ string tension, $\kappa_3=1$ GeV/fm, and not only by a factor 9/4.

Another piece of information about the strength of the gluon interaction which supports this observation comes from data on diffractive dissociation. The triple-Pomeron coupling turns out to be rather small [46]. If interpreted as a product of the Pomeron flux times the Pomeron-proton total cross section, the latter turns out to be an order of magnitude smaller than the proton-proton one. Naively one would again assume that the Pomeron as a colorless gluonic dipole should interact 9/4 times stronger that an analogous $\overline{qq}$ dipole (such a consideration led some authors to the conclusion that gluons are shadowed at small x in nuclei stronger than sea quarks). The only way to explain this discrepancy is to assume that the gluon-gluon dipole is much smaller. This, in turn, demands a stronger gluon-gluon interaction. Thus, diffraction is sensitive to nonperturbative interaction of gluons.

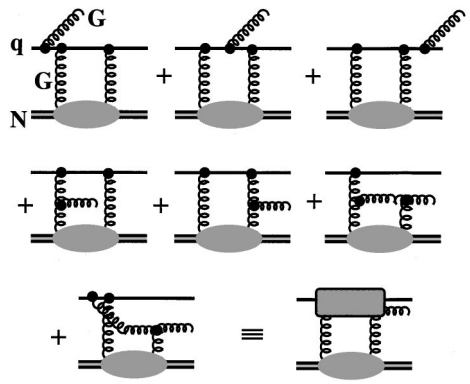

FIG. 2. Feynman diagrams for diffractive radiation of a gluon in a quark-nucleon interaction, $qN\to qGN$.

We shall use this observation in the next section to fix the corresponding parameters b_0 and b_1.

1. Diffractive bremsstrahlung of gluons. The triple-Pomeron coupling in the additive quark model

Let us start with diffractive dissociation of a quark, $qN\to qGN$. We assume the diffractive amplitude to be proportional to the gluon density $G(x,Q^2)=x\,g(x,Q^2)$ [56,57] (it should be a non-diagonal distribution if the energy is not very large) as is shown in Fig. 2. Since the amplitude is predominantly imaginary at high energies one can use the generalized unitarity relation known as Cutkosky rule [58],

$$2\,\mathrm{Im}\,A_{ab} = \sum_c A_{ac}A_{cb}^{\dagger}, \tag{59}$$

where A_{ab} is the amplitude of the process $a\to b$ and a, b denote all the particles in initial and final states respectively. In the case under discussion $a=\{q,N\}$, $b=\{q,G,N\}$, and c denotes either $c_1=\{q,N_8^*\}$ or $c_2=\{q,G,N_8^*\}$, where N_8^* is a color-octet excitation of the nucleon resulting from gluon radiation(absorption) by a nucleon.

In what follows, we concentrate on forward diffraction, i.e., the transverse momentum transfer $\vec{q}_T=0$. In this case the diffractive amplitude reads

$$F(\alpha,k_T,q_T=0) = \frac{i}{4\pi}\int\frac{d^2\rho}{2\pi}e^{i\vec{k}_T\vec{\rho}}\,\Psi_{qG}(\alpha,\vec{\rho})\,\tilde{\sigma}(\vec{\rho}), \tag{60}$$

where k_T is the transverse momentum of the radiated gluon and

$$\tilde{\sigma}(\vec{\rho}) = \frac{9}{8}\sigma_{qq}^{-}(\vec{\rho}). \tag{61}$$

Equation (60) is derived in Appendix A 2 in a simple and intuitive way based on the general properties of a diffractive process discussed in Appendix A 1. A more formal derivation based on a direct calculation of Feynman diagrams and the Cutkosky rule (59) is presented in Appendix B 1.

The relation (60) is valid for any value of α. In contrast to the inclusive cross section for gluon bremsstrahlung the diffractive cross section depends on α only via the distribution function.

The amplitude (60) is normalized according to

$$\frac{d\sigma(qN\to qGN)}{d(\ln\alpha)\,d^2k_T\,d^2q_T}=|F(\alpha,\vec{k}_T,\vec{q}_T)|^2. \tag{62}$$

The distribution for the effective mass squared, $M^2=k_T^2/\alpha(1-\alpha)\approx k_T^2/\alpha$, at $q_T=0$ has the form

$$\left.\frac{d\sigma(qN\to qGN)}{dM^2\,dq_T^2}\right|_{q_T=0}=2\pi^2\int_0^{M^2}dk_T^2\,|F(\alpha,\vec{k}_T,\vec{q}_T)|^2, \tag{63}$$

which transforms in the limit $M^2\to\infty$ into

$$\left.\frac{M^2\,d\sigma(qN\to qGN)}{dM^2\,dq_T^2}\right|_{q_T=0}=\frac{1}{16\pi}\lim_{\alpha\to 0}\int d^2\rho\,|\Psi_{qG}(\alpha,\vec{\rho})\,\tilde{\sigma}(\rho,\overline{s})|^2, \tag{64}$$

where $\overline{s}=M_0^2/\xi$, where $M_0^2=1$ GeV^2 and $\xi\equiv x_P\equiv 1-x_F\approx M^2/s$.

Since dissociation into large mass states is dominated by the triple-Pomeron (3P) graph the value on the LHS of Eq. (64) is the effective $3P$ coupling $G_{3P}(qN\to XN)$ (see definition in [46]) at $q_T=0$. It can be evaluated using $G_{3P}(pp\to Xp)\approx 1.5$ mb/GeV^2 as it follows from measurement by the CDF Collaboration [59] (according to [61][3] we divided the value of G_{3P} given in [59] by factor 2). This value is twice as small as one derived from the triple-Regge analyses [46] at medium large energies. This is supposed to be due to absorptive corrections which grossly diminish the survival probability of large rapidity gaps at high energies [60]. One can see energy dependence of G_{3P} even in the energy range of the CDF experiment [59].

Assuming the additive quark model (AQM) to be valid one can write

$$G_{3P}^{AQM}(qN\to XN)\approx\frac{1}{3}G_{3P}(NN\to XN)\approx 0.5\,\frac{\text{mb}}{\text{GeV}^2} \tag{65}$$

(see below about interference effects). To compare with this estimate we calculate the triple-Pomeron coupling (64) using the distribution function in the form (56) and the dipole cross section (30),

$$G_{3P}^{AQM}(qN\to XN)=\frac{27\alpha_s}{4}\left(\frac{\sigma_0}{8\pi}\right)^2\ln\left(\frac{t_1t_2}{t_3^2}\right), \tag{66}$$

[3]We thank Doug Jansen and Thomas Nunnemann who helped to clarify this point.

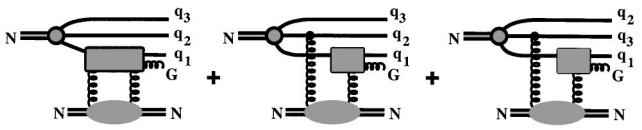

FIG. 3. Contributions from projectile valence quarks to the amplitude of diffractive gluon emission in NN collisions. Six additional graphs resulting from the permutation $\{1\rightleftharpoons 2\}$ and $\{1\rightleftharpoons 3\}$ have not been plotted.

where $t_1=b^2(0)/2$, $t_2=t_1+1/\rho_0^2$ and $t_3=2t_1t_2/(t_1+t_2)$. The parameters σ_0 and ρ_0 are defined in Eq. (30). We use here a fixed value of $\alpha_s=0.6$ which is an appropriate approximation for a soft process.

Comparison of Eq. (66) with the value (65) leads to a rough evaluation of the parameter b_0 of our potential (we are not sensitive to b_1 since we keep α small),

$$b^{AQM}(0)\approx 570\ \text{MeV}. \tag{67}$$

Thus a typical quark-gluon separation is $\sim 1/b(0)\approx 0.4$ fm what is roughly the radius of a ''constituent'' quark. Note that a substantial modification of Eq. (65) by interference of radiation amplitudes for different quarks is possible.

2. Diffractive excitation of nucleons, $NN\to XN$, beyond the AQM

The amplitude of diffractive gluon radiation $NN\to 3qGN$ can be represented as a superposition of radiation by different quarks as shown in Fig. 3. In this process the colorless $3q$ system ($|3q\rangle_1$) converts into a color-octet final state ($|3q\rangle_8$). There are two independent octet $|3q\rangle$ states which differ from each other by their symmetry under a permutation of the color indices of the quarks. Correspondingly, the amplitude for the process $NN\to|3q\rangle_8GN$ is a superposition of two amplitudes (see below).

The contribution to the amplitude of the first graph in Fig. 3 reads

$$F^I(NN\to 3qGN)=\frac{if_{abc}}{\sqrt{3}}\langle(3q)_8|\,\tau_b^{(1)}\,\tau_c^{(2)}|(3q)_1\rangle\,\tilde{\sigma}(\vec{\rho}_1)\times\Phi(\{\vec{r},\alpha\},\vec{\rho}_1,\alpha_G). \tag{68}$$

The second and third graphs in Fig. 3 give correspondingly,

$$F^{II}(NN\to 3qGN)=\frac{if_{abc}}{\sqrt{3}}\langle(3q)_8|\,\tau_b^{(1)}\,\tau_c^{(2)}|(3q)_1\rangle\times[\tilde{\sigma}(\rho_2)-\tilde{\sigma}(\vec{r}_1-\vec{r}_2)]\times\Phi(\{\vec{r},\alpha\},\vec{\rho}_1,\alpha_G); \tag{69}$$

and

$$F^{III}(NN\to 3qGN)=\frac{if_{abc}}{\sqrt{3}}\langle(3q)_8|\tau_b^{(1)}\,\tau_c^{(2)}|(3q)_1\rangle \times[\tilde{\sigma}(\rho_3)-\tilde{\sigma}(\vec{r}_1-\vec{r}_3)] \times\Phi(\{\vec{r},\alpha\},\vec{\rho}_1,\alpha_G). \tag{70}$$

Here $\{\vec{r},\alpha\}=(\vec{r}_1,\vec{r}_2,\vec{r}_3;\alpha_1\alpha_2,\alpha_3)$; $\vec{r}_i$ are the positions of the quarks in the impact parameter plane; $\vec{\rho}_i=\vec{\rho}-\vec{r}_i$, where $\vec{\rho}$ is the position of the gluon;

$$\Phi(\{\vec{r},\alpha\},\vec{\rho}_i,\alpha_G/\alpha_i)=\Psi_{N\to 3q}(\{\vec{r},\alpha\})\,\Psi_{Gq}(\vec{\rho}_i,\alpha_G); \tag{71}$$

f_{abc} is the structure constant of the color group, where ''a'' is the color index of the radiated gluon, and we sum over ''b'' and ''c.'' The Gell-Mann matrices $\lambda_c^i=2\,\tau_c^i$ act on the color index of ith quark.

Using the relation

$$f_{abc}\,\tau_b^{(1)}\,\tau_c^{(1)}\,|3q\rangle_1=f_{abc}\,(\tau_b^{(2)}\,\tau_c^{(1)}+\tau_b^{(3)}\,\tau_c^{(1)})\,|3q\rangle_1, \tag{72}$$

one can present the sum of the amplitudes F^I, F^{II} and F^{III} in the form

$$F^{(1)}(NN\to 3qGN)=F^I+F^{II}+F^{III} =\frac{if_{abc}}{\sqrt{3}}\Phi(\vec{r}_i,\alpha_i,\vec{\rho}-\vec{r}_1,\alpha_G) \times\langle(3q)_8|\tau_b^{(2)}\,\tau_c^{(1)}\,\Sigma_{12}+\tau_b^{(3)}\,\tau_c^{(1)}\,\Sigma_{13}| \times(3q)_1\rangle, \tag{73}$$

where $\Sigma_{ij}=\tilde{\sigma}(\vec{\rho}-\vec{r}_i)+\tilde{\sigma}(\vec{\rho}-\vec{r}_j)-\tilde{\sigma}(\vec{r}_i-\vec{r}_j)$. The index ''1'' in $F^{(1)}(NN\to 3qGN)$ indicates that the gluon is radiated by the quark q_1 in accordance with Fig. 3.

The amplitudes $F^{(2)}$ and $F^{(3)}$ is obviously related to $F^{(1)}$ by replacement $1\to 2,3$. Note that the color structure $f_{abc}\,\tau^{(2)}\,\tau^{(3)}$ which is not present in (73) is not independent due to the relation

$$f_{abc}(\tau_b^{(1)}\,\tau_c^{(2)}+\tau_b^{(2)}\,\tau_c^{(3)}+\tau_b^{(3)}\,\tau_c^{(1)})\,|3q\rangle_1=0. \tag{74}$$

Thus, we are left with only two independent color structures, as was mentioned above.

The full amplitude for diffractive gluon radiation squared $|F(NN\to 3qGN)|^2=|F^{(1)}+F^{(2)}+F^{(3)}|^2$, summed over all color states of the $3qG$ system, reads

$$\sum_f\,|F(NN\to 3qGN)|^2 =\frac{1}{3}|\Psi_{N\to 3q}(\{\vec{r},\alpha\})|^2\left\{\sum_{i=1}^{3}\,|\Psi_{qG}(\vec{\rho}_i,\alpha_G)|^2 \times A^{(i)}(\{\vec{r}\},\vec{\rho})-\mathrm{Re}\sum_{i\neq k}\,\Psi_{qG}(\rho_i,\alpha_G) \times\Psi_{qG}(\vec{\rho}_k,\alpha_G)\,B^{(i,k)}(\{\vec{r}\},\vec{\rho})\right\}, \tag{75}$$

where

$$A^{(1)}(\{\vec{r}\},\vec{\rho})=\Sigma_{12}^2+\Sigma_{13}^2+\Sigma_{12}\Sigma_{13}, \tag{76}$$

$$B^{(1,2)}(\{\vec{r}\},\vec{\rho})=2\,\Sigma_{12}^2+\Sigma_{12}(\Sigma_{13}+\Sigma_{23})-\Sigma_{13}\Sigma_{23}. \tag{77}$$

The expressions for $A^{(2)}$, $A^{(3)}$ and $B^{(1,3)}$, $B^{(2,3)}$ are obtained by simply changing the indices.

The effective triple-Pomeron coupling results from integrating Eq. (75) over phase space,

$$G_{3P}(NN\to NX)=\frac{1}{16\pi}\int d^2r_1\,d^2r_2\,d^2r_3\,d^2\rho\,d\alpha_1\,d\alpha_2\,d\alpha_3 \times\delta(\vec{r}_1+\vec{r}_2+\vec{r}_3)\,\delta(1-\alpha_1-\alpha_2-\alpha_3) \times\sum_f\,|F(NN\to 3qGN)|^2. \tag{78}$$

To evaluate $G_{3P}(NN\to NX)$ we use Eq. (19) for $\Psi_{qG}(\vec{\rho},\alpha)$ and a Gaussian parametrization for the valence quark distribution in the nucleon,

$$|\Psi_{N\to 3q}(\{\vec{r},\alpha\})|^2\propto\exp\left[-\left(\sum_{i=1}^{2}\,\vec{r}_i{}^2\right)\Big/\,\langle r_{ch}^2\rangle_p\right], \tag{79}$$

where $\langle r_{ch}^2\rangle_p\approx 0.79\pm 0.03$ fm^2 is the mean square radius of the proton [62]. At this point one has to introduce some specific model for the α_i distributions. Quite some proposals can be found in the literature, and a quantitative analysis will require careful numerical studies. For a first qualitative discussion we make the simple ansatz for the quark momentum distribution in the nucleon, $F_q^N(\alpha_1,\alpha_2,\alpha_3)\propto\Pi_i\delta(\alpha_i-1/3)$ which allows to continue our calculations analytically. The details of the integration of Eq. (78) can be found in Appendix C. G_{3P} is a function of the parameter $b(0)$. As a trial value we choose Eq. (67), $b(0)=570$ MeV, [estimated using the result of the additive quark model $G_{3P}(qN\to XN)\approx 0.5$ mb/GeV^2] we arrive at $G_{3P}(NN\to XN)\approx 2.4$ mb/GeV^2. This value is substantially higher than the experimental value $G_{3P}(NN\to XN)=1.5$ mb/GeV^2. This is an obvious manifestation of simplifying approximations (the quark additivity) we have done. In order to fit the experimental value of $G_{3P}(NN\to NX)$ after the contributions of the second and third graphs in Fig. 3 are included we should use in Eq. (78)

$$b(0)=650\ \mathrm{MeV}. \tag{80}$$

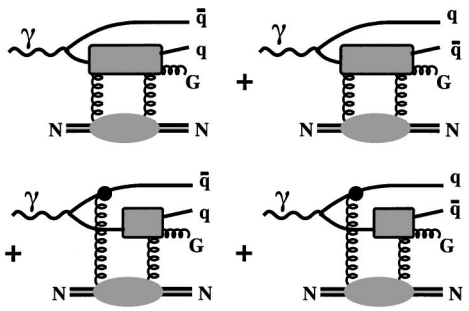

FIG. 4. Diagrams for the diffractive radiation of a gluon in photon-nucleon interaction, $\gamma^* N \to \bar{q}qGN$.

With this value Eq. (66) gives

$$G_{3P}(qN\to XN)\approx 0.3\frac{\mathrm{mb}}{\mathrm{GeV}^2}\approx\frac{1}{5}G_{3P}(NN\to XN), \quad (81)$$

which shows a substantial deviation from the AQM.

3. Diffractive gluon radiation by a (virtual) photon and mesons. Breakdown of Regge factorization

One can use a similar technique to calculate the cross section for diffractive gluon radiation by a photon and mesons. The diffraction amplitude $\gamma(M)N\to\bar{q}qGN$ is described by the four diagrams depicted in Fig. 4. The first two diagrams correspond to the AQM. In this approximation the forward ($q_T=0$) amplitude $\gamma N\to\bar{q}qGN$ reads

$$\begin{aligned}F^{AQM}(\gamma N\to\bar{q}qGN)&=\Psi^{-}_{qq}(\alpha,\vec{\rho}_1-\vec{\rho}_2)\,[F(qN\to qGN)-F(\bar{q}N\to\bar{q}GN)]\\&=\Psi^{-}_{qq}(\alpha,\vec{\rho}_1-\vec{\rho}_2)\left[\Psi_{qG}\left(\frac{\alpha_G}{\alpha},\vec{\rho}_1\right)\tilde{\sigma}(\rho_1)\right.\\&\quad\left.-\Psi^{-}_{qG}\left(\frac{\alpha_G}{1-\alpha},\vec{\rho}_2\right)\tilde{\sigma}(\rho_2)\right],\end{aligned} \quad (82)$$

where $\vec{\rho}_i=\vec{\rho}-\vec{r}_i$ (i=1,2). $\vec{\rho},\vec{r}_{1,2}$ are the radius-vectors of the gluon, quark and antiquark, respectively. The limit $\alpha_G\to 0$ is assumed.

After addition of the last two graphs in Fig. 4 the amplitude takes the form (we do not write out its trivial color structure),

$$\begin{aligned}F(\gamma N\to\bar{q}qGN)&=\Psi^{-}_{qq}(\alpha,\vec{\rho}_1-\vec{\rho}_2)\left[\Psi_{qG}\left(\frac{\alpha_G}{\alpha},\vec{\rho}_1\right)-\Psi^{-}_{qG}\left(\frac{\alpha_G}{1-\alpha},\vec{\rho}_2\right)\right]\\&\quad\times[\tilde{\sigma}(\rho_1)+\tilde{\sigma}(\rho_2)-\tilde{\sigma}(\vec{\rho}_1-\vec{\rho}_2)].\end{aligned} \quad (83)$$

The detailed calculation of the diagrams depicted in Fig. 4 is presented in Appendix B 2. A much simpler and more intuitive derivation of Eq. (83) is suggested in Appendix A 3.

If one neglects the nonperturbative effects in Eq. (83) [$b(\alpha)=0$] this expression coincides with Eq. (3.4) in [19], but is quite different from the cross section of diffractive gluon radiation derived in [18] [Eq. (60)] (see footnote 1). A crucial step in [18] is the transition from Fock states which are the eigenstates of interaction, to the physical state basis. Such a rotation of the *S*-matrix leads to a renormalization of the probability *amplitudes* for the Fock states (see Appendix A 1), rather than just the probabilities as it was assumed in [18].

The amplitude (83) is normalized as

$$\left.\frac{d\sigma}{d(\ln\alpha_G)\,dq_T^2}\right|_{q_T=0}=\frac{1}{16\pi}\int d^2\rho_1\,d^2\rho_2 d\alpha\times|F(\gamma N\to\bar{q}qGN)|^2. \quad (84)$$

Direct comparison of of the cross section for diffractive gluon radiation by a photon calculated with this expression with data is complicated by contribution of diffraction to $\bar{q}q$ states and nondiffractive (Reggeon) mechanisms. This is why one should first perform a detailed triple-Regge analysis of data and then to compare Eq. (84) with the effective triple-Pomeron coupling. Good data for photon diffraction are available at lab. energy $E_\gamma=100$ GeV [63]. At this energy, however, there is no true triple-Regge region which demands $s/M^2\gg 1$ and $M^2\gg 1$ GeV^2. Therefore the results of the triple-Regge analysis in [63] cannot be trusted. It is much more appropriate to use available data from the DESY *ep* collider HERA, particularly those in [64] at $\sqrt{s}=200$ GeV where a triple-Regge analysis taking into account four graphs was performed. The result for the effective triple-Pomeron coupling

$$G_{3P}^{\gamma p}(0)=(8.19\pm 1.6\pm 1.34\pm 2.22)\ \mu\mathrm{b/GeV}^2 \quad (85)$$

should be compared with our prediction $G_{3P}^{\gamma p}(0)=9\ \mu$b/GeV^2. To estimate the mean energy for the dipole cross section $\bar{s}/M^2$ GeV^2 we used the midvalue $M^2=250$ GeV^2 of the interval of M^2 measured in [64] which corresponds to $x_P=0.0064$. Thus, high-energy data for gluon radiation in diffractive dissociation of protons and photons give the value (80) for the parameter of nonperturbative quark-gluon interaction.

Note that the relative role of ''additive'' (Nos. 1,2 in Fig. 4 and No. 1 in Fig. 3) and ''non-additive'' (Nos. 3,4 in Fig. 4 and Nos. 2,3 in Fig. 3) graphs depends on the relation between the three characteristic sizes $R_h=\sqrt{\langle r_{ij}^2\rangle}$, ρ_0 and $1/b(0)$. In the limit $R_h\gg\rho_0$, $1/b(0)$ the contribution of the ''nonadditive'' graphs vanishes and the additive quark model becomes a good approximation. However, at realistic values of $R_h\sim 1$ fm the ''additive'' and ''non-additive'' contributions are of the same order and the latter becomes dominant for small R_h. Particularly, this explains why the factorization relation,

$$A_{3P}(hN\to XN)=\frac{G_{3P}(hN\to XN)}{\sigma_{tot}(hN)}=\mathrm{const}, \quad (86)$$

i.e., independent of *h*, is substantially broken. We expect

$$A_{3P}(NN\to XN)=0.025\ \ \mathrm{GeV}^{-2},$$

$$A_{3P}(\pi N\to XN)=0.031\ \ \mathrm{GeV}^{-2},$$

$$A_{3P}(KN\to XN)=0.042\ \ \mathrm{GeV}^{-2},$$

$$A_{3P}(\gamma N\to XN)=0.052\ \ \mathrm{GeV}^{-2}. \tag{87}$$

We see that our predictions for the triple-Pomeron vertex as defined from diffractive dissociation of nucleons and photons are different by almost factor of three. On top of that, the absorptive corrections which are known to be larger for diffraction than for elastic scattering also contribute to the breaking of Regge factorization. A manifestation of these correction shows up as deviation between the data and the Regge based expectations for the energy dependence of the diffractive cross section [61,65].

B. Gluon shadowing in nuclei

It is known since long time [66] that the parton distribution in nuclei is shadowed at small x due to parton fusion. In QCD this effect corresponds to the nonlinear term in the evolution equation responsible for gluon recombination [21,67]. This phenomenon is very important as soon as one calculates the cross section of a hard reaction (gluon radiation with high k_T, prompt photons, Drell-Yan reaction, heavy flavor production, etc.) assuming factorization. Nuclear shadowing of sea quarks is well measured in DIS, but for gluons it is poorly known. One desperately needs to know it to provide predictions for the high-energy nuclear colliders, the BNL Relativistic Heacy Ion Collider (RHIC) and CERN Large Hadron Collider (LHC).

The interpretation of nuclear shadowing depends on the choice of the reference frame. In the infinite momentum frame of the nucleus it looks like parton fusion. Indeed, the longitudinal spread of the valence quarks in the bound nucleons, as well as the internucleon distances, are subject to Lorentz contraction. Therefore the nucleons are spatially well separated. However, the longitudinal spread of partons at small x contracts much less because they have an x times smaller Lorentz factor. Therefore, such partons can overlap and fuse even if they originate from different nucleons [66]. Fusion of two gluons into a $\overline{q}q$ pair leads to shadowing of sea quarks. If two gluons fuse to a single gluon it results in shadowing of gluons.

The same phenomenon looks quite differently in the rest frame of the nucleus, as shadowing of long-living hadronic fluctuations of the virtual photon. This resembles the ordinary nuclear shadowing for the total cross sections of hadron-nucleus interaction. Indeed, the total virtual photoabsorption cross section is proportional to the structure function $F_2(x,Q^2)$. However, one can calculate in this way only shadowing of quarks. To predict shadowing of gluons it was suggested in [68] to replace the photon by a hypothetical particle probing gluons. Assuming for the GG fluctuation of this particle the same distribution function as for $\overline{q}q$ one may conclude that the effective absorption cross section providing shadowing is 9/4 times larger than for a $\overline{q}q$ fluctuation of a photon. Such a simple result cannot be true because of the strong gluon-gluon interaction which makes their distribution function quite different (''squeezes'' it). Besides, the spin structure of the GG distribution function is different too.

1. Nuclear shadowing for longitudinal photons

Longitudinally polarized photons are known to be a good probe for the gluon structure function. Indeed, the aligned jet model [2] cannot be applied in this case since the distribution function for longitudinal photons (1),(4) suppresses the asymmetric $\overline{q}q$ fluctuations with $\alpha\to 0,1$. Therefore, the transverse separation of the $\overline{q}q$ pair is small $\sim 1/Q^2$ and nuclear shadowing can be only due to shadowing of gluons. One can also see that from the expression for the cross section of a small size dipole [56,57],

$$\sigma_{qq}^{A,N}(r_T,x)\approx\frac{\pi^2}{3}\alpha_s(Q^2)\,G_N(x,Q^2), \tag{88}$$

where $G_N(x,Q^2)=x\,g(x,Q^2)$ is the gluon density and $Q^2\sim 1/r_T^2$. Thus, we expect nearly the same nuclear shadowing at large Q^2 for the longitudinal photoabsorption cross section and for the gluon distribution,

$$\frac{\sigma_A^L(x,Q^2)}{\sigma_N^L(x,Q^2)}\approx\frac{G_A(x,Q^2)}{G_N(x,Q^2)}. \tag{89}$$

The estimate for nuclear shadowing for longitudinally polarized photons follows.

Nuclear shadowing for photons corresponds to the inelastic nuclear shadowing as it was introduced for hadrons by Gribov 30 years ago [33]. Therefore, the term $\Delta\sigma(\gamma^*A)=\sigma_{tot}(\gamma^*A)-A\,\sigma(\gamma^*N)$ representing shadowing in the total photoabsorption cross section is proportional to the diffractive dissociation cross section $\gamma^*N\to XN$ [33,69], considered above. In the lowest order in the intensity of XN interaction the shadowing correction reads

$$\Delta\sigma(\gamma^*A)=8\pi\,\mathrm{Re}\int d^2b\int dM_X^2 \times\left.\frac{d^2\sigma(\gamma^*N\to XN)}{dM_X^2\,dq_T^2}\right|_{q_T=0} \times\int_{-\infty}^{\infty}dz_1\int_{-\infty}^{\infty}dz_2\,\Theta(z_2-z_1)\,\rho_A(b,z_1)\,\rho_A(b,z_2) \times\exp[-i\,q_L\,(z_2-z_1)], \tag{90}$$

where

$$q_L=\frac{Q^2+M_X^2}{2\,\nu}. \tag{91}$$

Here ν is the photon energy; z_1 and z_2 are the longitudinal coordinates of the nucleons N_1 and N_2, respectively, participating in the diffractive transition $\gamma^*N_1\to XN_1$ and back $XN_2\to\gamma^*N_2$.

The longitudinal momentum transfer (91) controls the lifetime (coherence time t_c) of the hadronic fluctuation of the photon, $t_c=1/q_L$. It is known only if the mass matrix is diagonal, i.e., the fluctuations have definite masses. However, in this case the interaction cross section of the fluctuation has no definite value. Then one faces a problem of calculation of nuclear attenuation for the intermediate state X via interaction with the nuclear medium.

This problem can be settled using the Green function formalism developed above in Sec. II A [12,14]. One should switch to the quark-gluon representation for the produced state $X=|\overline{q}q\rangle$, $|\overline{q}qG\rangle$, $|\overline{q}q2G\rangle$, ... As one can see below an exact solution is not an easy problem even for the two lowest Fock states. For higher states containing two or more gluons it may be solved in the double-leading-log approximation which neglects the size of the previous Fock state and treats a multi-gluon fluctuation as a color octet-octet dipole. This is actually what we do in what follows, except the Fock state with only one gluon leads to a $1/M^2$ mass distribution for diffraction, while inclusion of multi-gluon components makes it slightly steeper. This is not a big effect, besides, the nuclear formfactor substantially cuts off the reachable mass interval (see below). Therefore, we restrict the following consideration by the first two Fock states.

For the lowest state $|\overline{q}q\rangle$ one can write

$$\begin{aligned}
&8\pi\,\mathrm{Re}\int dM_X^2\,\frac{d^2\sigma(\gamma^*N\to XN)}{dM_X^2\,dq_T^2}\bigg|_{q_T=0}\exp[-i\,q_L\,(z_2-z_1)]\\
&=\frac{1}{2}\,\mathrm{Re}\int d^2k_T\int_0^1 d\alpha\,|F_{\gamma^*\to\overline{q}q}(\vec{k}_T,\alpha)|^2\exp\left[-i\,\frac{\epsilon^2+k_T^2}{2\,\nu\,\alpha(1-\alpha)}(z_2-z_1)\right]\\
&\equiv\frac{1}{2}\,\mathrm{Re}\int d^2r_1\,d^2r_2\int_0^1 d\alpha\;\;F^{\dagger}_{\gamma^*\to\overline{q}q}(\vec{r}_2,\alpha)\,G^0_{\overline{q}q}(\vec{r}_2,z_2;\vec{r}_1,z_1)\,F_{\gamma^*\to\overline{q}q}(\vec{r}_1,\alpha),
\end{aligned} \tag{92}$$

where ϵ was defined in Eq. (3).

The amplitudes of diffraction $\gamma^*N\to XN$ in the transverse momentum and coordinate representations are related by Fourier transform:

$$F_{\gamma^*\to\overline{q}q}(\vec{k}_T,\alpha)=\frac{1}{2\pi}\int d^2r\,F_{\gamma^*\to\overline{q}q}(\vec{r}_1,\alpha)\,e^{i\,\vec{k}_T\cdot\vec{r}}. \tag{93}$$

This amplitude in the coordinate representation has a factorized form

$$F_{\gamma^*\to\overline{q}q}(\vec{r}_1,\alpha)=\Psi^{\overline{q}q}(\vec{r},\alpha)\,\sigma^{\overline{q}q}(r). \tag{94}$$

$G^0_{\overline{q}q}(\vec{r}_2,z_2;\vec{r}_1,z_1)$ in Eq. (92) is the Green function of a free propagation of the $\overline{q}q$ pair between points z_1 and z_2. It is a solution of Eq. (7) without interaction

$$G^0_{\overline{q}q}(\vec{r}_2,z_2;\vec{r}_1,z_1)=\frac{1}{(2\pi)^2}\int d^2k_T\exp\left[-i\,\vec{k}_T\cdot(\vec{r}_2-\vec{r}_1)-\frac{i\,k_T^2(z_2-z_1)}{2\,\nu\,\alpha(1-\alpha)}\right]. \tag{95}$$

The boundary condition for the Green function is

$$G^0_{\overline{q}q}(\vec{r}_2,z_2;\vec{r}_1,z_1)|_{z_2=z_1}=\delta(\vec{r}_2-\vec{r}_1). \tag{96}$$

In Eq. (95) the phase shift on the distance z_2-z_1 is controlled by the transverse momentum squared as one could expect from Eqs. (90),(91) where it depends on the M_X^2. However, Eq. (92) is written now in the coordinate representation and contains no uncertainty with the absorption cross section, as different from Eq. (90). In order to include the effects of absorption of the intermediate state X into Eq. (92) one should replace the free Green function $G^0_{\overline{q}q}(\vec{r}_2,z_2;\vec{r}_1,z_1)$ by the solution of the Schrödinger equation (7) with imaginary potential (9). This was done in paper [12] and the results have demonstrated a substantial deviation of nuclear shadowing from usually used approximations for transverse

photons. One should also include the real part of the potential which takes into account the nonperturbative interaction between q and $\bar{q}$ as it is described in Sec. II A. This is important only for nuclear shadowing of transverse photons and and low Q^2 longitudinal photons and is beyond the scopes of present paper. Therefore, we skip further discussion of nuclear shadowing for the $|\bar{q}q\rangle$ pair and switch to the next Fock component $|\bar{q}qG\rangle$.

For the intermediate state (44) $X=\bar{q}qG$ Eq. (92) is modified as

$$8\pi\int dM_X^2\,\frac{d^2\sigma(\gamma^*N\to XN)}{dM_X^2\,dq_T^2}\bigg|_{q_T=0}\cos[q_L(z_2-z_1)]$$

$$\Rightarrow\frac{1}{2}\mathrm{Re}\int d^2x_2\,d^2y_2\,d^2x_1\,d^2y_1\int d\alpha_q\,d\ln(\alpha_G)F^{\dagger}_{\gamma^*\to\bar{q}qG}(\vec{x}_2,\vec{y}_2,\alpha_q,\alpha_G)$$

$$\times G^{-}_{\bar{q}qG}(\vec{x}_2,\vec{y}_2,z_2;\vec{x}_1,\vec{y}_1,z_1)F_{\gamma^*\to\bar{q}qG}(\vec{x}_1,\vec{y}_1,\alpha_q,\alpha_G),\tag{97}$$

where α_q and α_G are the fractions of the photon light cone momentum carried by the quark and gluon, respectively. The amplitude of diffraction $\gamma^*N\to XN$ depends on the q-$\bar{q}$ transverse separation $\vec{x}$ and the distance $\vec{y}$ from the gluon to the center of gravity of the $\bar{q}q$ pair (we switch to these variables from the previously used $\vec{\rho}_{1,2}$ for the sake of convenience, it simplifies the expression for kinetic energy).

The Schrödinger equation for the Green function $G^{-}_{\bar{q}qG}$ describing propagation of the $\bar{q}qG$ system through a medium including interaction with the environment as well as between the constituent has the form

$$i\frac{d}{dz_2}\;G^{-}_{\bar{q}qG}(\vec{x}_2,\vec{y}_2,z_2;\vec{x}_1,\vec{y}_1,z_1)$$

$$=\left\{\frac{Q^2}{2\nu}-\frac{\alpha_q+\alpha_{\bar{q}}}{2\nu\alpha_q\alpha_{\bar{q}}}\Delta(\vec{x}_2)-\frac{1}{2\,\nu\,\alpha_G(1-\alpha_G)}\Delta(\vec{y}_2)\right.$$

$$\left.+V(\vec{x}_2,\vec{y}_2,z_2,\alpha_q,\alpha_G)\right\}$$

$$\times G^{-}_{\bar{q}qG}(\vec{x}_2,\vec{y}_2,z_2;\vec{x}_1,\vec{y}_1,z_1),\tag{98}$$

with the boundary condition,

$$G^{-}_{\bar{q}qG}(\vec{x}_2,\vec{y}_2,z_2;\vec{x}_1,\vec{y}_1,z_1)|_{z_2=z_1}=\delta(\vec{x}_2-\vec{x}_1)\;\delta(\vec{y}_2-\vec{y}_1).\tag{99}$$

The imaginary part of the potential $V(\vec{x}_2,\vec{y}_2,z_2,\alpha_q,\alpha_G)$ in Eq. (98) is proportional to the interaction cross section for the $\bar{q}qG$ system with a nucleon,

$$2\,\mathrm{Im}\,V(\vec{x}_2,\vec{y}_2,z_2,\alpha_q,\alpha_G)$$

$$=\left\{\frac{1}{8}\,\sigma^{-}_{\bar{q}q}(\vec{x})-\frac{9}{8}\left[\sigma^{-}_{\bar{q}q}\left(\vec{y}-\frac{\alpha^{-}_{\bar{q}}}{1-\alpha_G}\vec{x}\right)\right.\right.$$

$$\left.\left.+\sigma^{-}_{\bar{q}q}\left(\vec{y}-\frac{\alpha^{-}_{\bar{q}}}{1-\alpha_G}\vec{x}\right)\right]\right\}\rho_A(b,z).\tag{100}$$

The real part of this potential responsible for the nonperturbative interaction between the quarks and gluon is discussed below.

If the potential $\mathrm{Im}\,V(\vec{x}_2,\vec{y}_2,z_2,\alpha_q,\alpha_G)$ is a bi-linear function of $\vec{x}$ and $\vec{y}$ then Eq. (98) can be solved analytically. Nevertheless, the general case of nuclear shadowing for a three-parton system is quite complicated and we should simplify the problem.

Let us consider nuclear shadowing for longitudinally polarized photons with high Q^2. The latter means that one can neglect the eikonal attenuation for the $\bar{q}q$ Fock component of the longitudinal photon, i.e.,

$$Q^2\gg 4C\,\langle T_A\rangle\approx 1\ \mathrm{GeV}^2,\tag{101}$$

where C is the factor in Eq. (5) and $\langle T_A\rangle$ is the mean nuclear thickness function.

As different from the case of transversely polarized photons which distribution function (1)–(3) contains $\bar{q}q$ pairs with large separation ($\alpha\to 0,1$) even at large Q^2, in longitudinally polarized photons small size ($\sim 1/Q$) $\bar{q}q$ pairs always dominate [1,2]. This property suggest a few simplifications for the following calculations.

(1) One can neglect at large Q^2 the nonperturbative $\bar{q}q$ interaction and use the perturbative photon wave function (1)–(4).

(2) One can simplify the expression for the diffractive amplitude $\gamma^* N \to \bar{q}qGN$ introduced in Eq. (97) relying on smallness of the typical $\bar{q}q$ separation $|\vec{x}| \sim 1/Q$ in comparison with the distance between the $\bar{q}q$ and the gluon $|\vec{y}| \sim 1/b_0 \approx 0.3$ fm.

(3) One can also simplify Eq. (98) for the Green function $G_{\bar{q}qG}$ fixing $\vec{x}=0$ in the expression (99) for the nonperturbative potential $\mathrm{Im}\, V(\vec{x}_2,\vec{y}_2,z_2,\alpha_q,\alpha_G)$. This leads in Eq. (98) to a factorized dependence on variables $\vec{x}$ and $\vec{y}$.

As a result of these approximations and $\alpha_G \to 0$ we arrive at

$$F_{\gamma^* \to \bar{q}qG}(\vec{x},\vec{y},\alpha_q,\alpha_G) = -\Psi^L_{\bar{q}q}(\vec{x},\alpha_q)\, \vec{x}\cdot\vec{\nabla}\, \Psi_{qG}(\vec{y})\, \sigma_{\bar{G}G}(\vec{y}), \tag{102}$$

where

$$\Psi_{qG}(\vec{y}) = \lim_{\alpha_G \to 0} \Psi_{qG}(\alpha_G,\vec{y}), \tag{103}$$

and

$$\sigma_{GG}(r,s) = \frac{9}{4}\sigma_{\bar{q}q}(r,s). \tag{104}$$

As soon as we neglect the size of the color-octet $\bar{q}q$ pair, it interacts a gluon, this is why one can replace $\sigma_{\bar{q}qG}$ by the dipole cross section σ_{GG}. The latter is larger than $\sigma_{\bar{q}q}$ by the Casimir factor 9/4.

In this case the tree-body Green function factorizes to a product of two-body ones,

$$G_{\bar{q}qG}(\vec{x}_2,\vec{y}_2,z_2;\vec{x}_1,\vec{y}_1,z_1) \Rightarrow G_{\bar{q}q}(\vec{x}_2,z_2;\vec{x}_1,z_1) G_{GG}(\vec{y}_2,z_2;\vec{y}_1,z_1), \tag{105}$$

where $G_{\bar{q}q}(\vec{x}_2,z_2;\vec{x}_1,z_1)$ is the ''free'' Green function of the $\bar{q}q$ pair, and $G_{GG}(\vec{y}_2,z_2;\vec{y}_1,z_1)$ describes propagation of the GG dipole which constituents interact with each other, as well as with the nuclear medium.

$$i\frac{d}{d z_2}\, G_{GG}(\vec{y}_2,z_2;\vec{y}_1,z_1) = \left[-\frac{\Delta(\vec{y}_2)}{2\nu\alpha_G(1-\alpha_G)} + V(\vec{y}_2,z_2)\right] G_{GG}(\vec{y}_2,z_2;\vec{y}_1,z_1), \tag{106}$$

where

$$2\,\mathrm{Im}\, V(\vec{y},z) = -\sigma_{GG}(\vec{y})\,\rho_A(b,z). \tag{107}$$

On analogy to Eq. (11) we assume the real part of the potential has a form

$$\mathrm{Re}\, V(\vec{y},z) = \frac{\tilde{b}^4 y^2}{2\,\nu\,\alpha_G(1-\alpha_G)}, \tag{108}$$

where $\tilde{b} \sim b_0$.

To simplify the estimate we assume that $\sigma_{GG}(r,s) \approx C_{GG}(s)\, r^2$, where $C_{GG}(s) = d\,\sigma_{GG}(r,s)/d\, r^2_{r=0}$.

The solution of Eq. (106) has a form

$$G_{GG}(\vec{y}_2,z_2;\vec{y}_1,z_1) = \frac{A}{2\pi \sinh(\Omega\,\Delta z)} \times \exp\left\{ -\frac{A}{2}\left[(y_1^2+y_2^2)\coth(\Omega\,\Delta z) - \frac{2\vec{y}_1\cdot\vec{y}_2}{\sinh(\Omega\,\Delta z)}\right]\right\}, \tag{109}$$

where

$$A = \sqrt{\tilde{b}^4 - i\alpha_G(1-\alpha_G)\,\nu C_{GG}\,\rho_A}$$

$$\Omega = \frac{iA}{\alpha_G(1-\alpha_G)\,\nu}$$

$$\Delta z = z_2 - z_1. \tag{110}$$

The quark-gluon wave function in Eq. (102) has a form similar to Eq. (27),

$$\Psi_{qG}(\vec{y}) = \frac{2}{\pi}\sqrt{\frac{\alpha_s}{3}}\,\frac{\vec{e}\cdot\vec{y}}{y^2}\exp\left[-\frac{b^2}{2}y^2\right]. \tag{111}$$

Now we have all the components of the amplitude (102) which we need to calculate the nuclear shadowing correction (97). Integration in $\vec{x}_{1,2}$ and $\vec{y}_{1,2}$ can be performed analytically:

$$8\pi\int dM_X^2\,\frac{d^2\sigma(\gamma^*N\to XN)}{dM_X^2\,dq_T^2}\bigg|_{q_T=0}\cos(q_L\,\Delta z)$$

$$=\mathrm{Re}\int d\alpha_q\,d\ln(\alpha_G)\,\frac{16\,\alpha_{em}\left(\sum_F Z_q^2\right)\alpha_s(Q^2)\,C_{GG}^2}{3\,\pi^2\,Q^2\,\tilde{b}^2}[(1-2\,\zeta-\zeta^2)\,e^{-\zeta}+\zeta^2\,(3+\zeta)\,\mathrm{E}_1(\zeta)]$$

$$\times\left[\frac{t}{w}+\frac{\sinh(\Omega\,\Delta z)}{t}\ln\left(1-\frac{t^2}{u^2}\right)+\frac{2\,t^3}{u\,w^2}+\frac{t\sinh(\Omega\,\Delta z)}{w^2}+\frac{4\,t^3}{w^3}\right], \tag{112}$$

where

$$\zeta=ixm_N\Delta z;$$

$$t=\frac{A}{\tilde{b}^2};$$

$$u=t\cosh(\Omega\,\Delta z)+\sinh(\Omega\,\Delta z);$$

$$w=(1+t^2)\sinh(\Omega\Delta z)+2\,t\cosh(\Omega\Delta z). \tag{113}$$

The rest integration in Eq. (112) can be performed numerically. We calculated the ratio $R_{A/N}^G=G_A(x,Q^2)/a\,G_N(x,Q^2)$ for the gluon distribution functions for small values of Bjorken $10^{-4}<x<10^{-1}$ and high $Q^2=10$ GeV^2. We found $R_{A/N}^G$ almost independent of Q^2 at higher Q^2. The results are depicted in Fig. 5.

One can see that in contrast to the quark distribution the onset of nuclear shadowing for gluons starts at quite small $x\sim10^{-2}$. This is because the photon fluctuations containing gluons are heavier than $\bar{q}q$ fluctuations. Correspondingly, the lifetime of such fluctuations is shorter (or q_L is smaller) and they need a smaller x to expose coherent effects like nuclear shadowing. One can expect an antishadowing effect at medium $x\sim0.1$ like in $F_2(x,Q^2)$ which should push the crossing point $G_A(x,Q^2)/G_N(x,Q^2)=1$ down to smaller x. Discussion of the dynamics of antishadowing (swelling of bound nucleons, etc.) goes beyond the scopes of this paper.

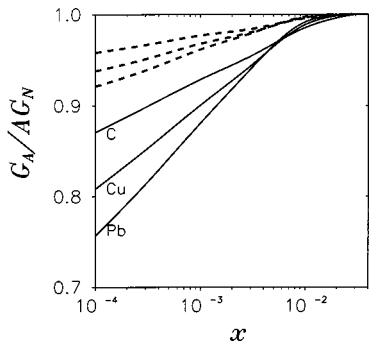

FIG. 5. Ratio of the gluon distribution functions in nuclei (carbon, copper and lead) and nucleons at small Bjorken x and $Q^2=4$ GeV^2 (solid curves) and 40 GeV^2 (dashed curves).

A similar approach to the problem of gluon shadowing is developed in [30] which relates shadowing to the diffractive radiation of gluons. Note that a delayed onset of gluon shadowing (at $x<0.02$) is also expected in [30]. However, this is a result of an *ad hoc* parametrization for antishadowing, rather than calculations. The phase shift factor $\cos(q_L\Delta z)$ which controls the onset of shadowing in Eqs. (97),(112) is neglected in [30] assuming that x is sufficiently small. However, nuclear shadowing for gluons does not saturate even at very small x because of the $1/M^2$ form of the mass dependence of diffractive radiation of gluons (triple-Pomeron diffraction). The smaller the $x=Q^2/2m_N\nu$ is, the higher masses are allowed by the nuclear form factor $[q_L=(Q^2+M^2)/2\nu<1/R_A]$ to contribute to the shadowing.

Our results also show that $R_{A/N}^G$ steeply decreases down to small x and seems to have a tendency to become negative. It would not be surprising for heavy nuclei if our shadowing correction corresponded to double scattering term only. However, the expression (97) includes all the higher order rescattering terms. The source of the trouble is the obvious breaking down of the unitarity limit $\sigma_{diff}<\sigma_{tot}$. This problem is well known and easily fixed by introducing the unitarity or absorptive corrections which substantially slow down the growth of the diffractive cross section. Available data for diffraction $pp\to pX$ clearly demonstrate the effect of unitarity corrections [61,65]. One may expect that at very high energies the relative fraction of diffraction decreases. We restrict ourselves with this word of caution in the present paper and postpone a further study of unitarity effects for a separate publication, as well as the effects of higher Fock components containing more than one gluon. Those corrections also become more important at small x.

Note that quite a strong nuclear suppression for gluons $G^A(x,Q^2)/G^N(x,Q^2)<F_2^A(x,Q^2)/F_2^N(x,Q^2)$ was predicted in [68] basing on the fact that the cross section of a color octet-octet dipole contains the factor 9/4 compared to σ_{qq}^-. However, it is argued above in Sec. III A and confirmed by the following calculations that the observed smallness of the diffractive cross section of gluon radiation shows that that the strong nonperturbative interaction of gluons substantially reduces the size of fluctuations including the gluon. The situation is much more complicated and cannot be reduced to a simple factor 9/4.

A perspective method for calculation of nuclear shadowing for gluons was suggested in the recent publication [31]. Experimental data for diffractive charm production can be used to estimate the effect. This seems to be more reliable than pure theoretical calculations performed above. Indeed, the transverse separation of a heavy flavored $\overline{Q}Q$ pair is small even at low Q^2, and may be assumed to be much smaller that the mean distance between the $\overline{Q}Q$ and the gluon. Unfortunately, the available data obtained at HERA have quite poor accuracy. The results from H1 [71] and ZEUS [72] experiments are different by almost factor of two. Besides, the theoretical analysis [34,35] which is needed to reconstruct the diffractive cross section of charm production from production of D^* in a limited phase space, introduces substantial uncertainty. According to [35] the realistic solutions for the diffractive charm production differ by a factor of five. In this circumstances we suppose our calculation for nuclear shadowing of gluons seems to be more reliable.

Note that we expect much weaker nuclear shadowing for gluons than it was predicted in [27,29,30]. For instance at $x=10^{-3}$ and $Q^2=4$ GeV^2 we expect $G_A/A\,G_N\approx 0.9$, while a much stronger suppression $G_A/A\,G_N\approx 0.6$ [27], even $G_A/A\,G_N\approx 0.3$ [29,30] was predicted for $A\approx 200$ at $Q^2=4$ GeV^2.

It is instructive to compare the gluon shadowing at high Q^2 with what one expects for hadronic reactions at much smaller virtualities. One should expect more shadowing at smaller Q^2, however, the soft gluon shadowing evaluated in the next section turns out to be much weaker than one predicted in [27,29,30] at high Q^2.

At the same time, quite a different approach to the problem of gluon shadowing based on the nonlinear GLR evolution equation [21] used in [26] led to the results pretty close to ours.

2. Nuclear shadowing for soft gluons

(i) Hadronic diffraction and gluon shadowing. The hadron-nucleus total cross section is known to be subject to usual Glauber (eikonal) [73] shadowing and Gribov's inelastic corrections [33]. Those corrections are controlled by the cross section of diffractive dissociation of the projectile hadron $hN\to XN$ which contains particularly the triple-Pomeron contribution. The latter as was shown above is related to gluon shadowing in nuclei. Namely, absorption of the incoming hadron can be treated as a result of interaction with the gluon cloud (in the infinite momentum frame of the nucleus) of bound nucleons at small x. A substantial part of this absorption is reproduced by the eikonal approximation which assumes the gluon density to be proportional to the number of bound nucleons. However, evolution of the gluon density including gluon fusion (see [66] and [21,67] for high Q^2) results in reduction of the gluon density compared to one used in the eikonal approximation. Such a reduction makes nuclear matter more transparent for protons [75–77].

That part of nuclear shadowing which comes from diffractive excitation of the valence quark component of the projectile hadron corresponds in terms of the triple-Regge phenomenology to the PPR term in the diffractive cross section. In eigenstate representation for the interaction Hamiltonian the same effect comes from the dependence of the elastic amplitude on positions of the valence quarks in the impact parameter plane [5]. On top of that, the projectile hadron can dissociate via gluon radiation which corresponds to the triple-Pomeron term in diffraction. It can also be interpreted in the infinite momentum frame of the nucleus as a reduction of the density of gluons which interact with the hadron. This relation gives a hint how to approach the problem of gluon shadowing at small x for soft gluons.

Let us model this situation in eigenstate representation with two Fock states for the projectile hadron,

$$|h\rangle=(1-w)|h\rangle_v+w|h\rangle_G\,, \tag{114}$$

where $|h\rangle_v$ and $|h\rangle_G$ are the components without (only valence quarks) and with gluons which can be resolved at the soft scale. We assume them to be eigenstates of interaction with eigenvalues σ_v and σ_G respectively. The relative weights are controlled by the parameter w. The hadron-nucleon and hadron-nucleus total cross sections can be represented as [74,5],

$$\sigma_{tot}^{hN}=\sigma_v+w\Delta\sigma, \tag{115}$$

where $\Delta\sigma=\sigma_G-\sigma_v$, and

$$\sigma_{tot}^{hA}=2\int d^2b\left\{\left[1-\exp\left(-\frac{1}{2}\sigma_v\,T(b)\right)\right]+w\left[\exp\left(-\frac{1}{2}\sigma_v\,T(b)\right)-\exp\left(-\frac{1}{2}\sigma_G\,T(b)\right)\right]\right\}. \tag{116}$$

This cross section is smaller than one given by the eikonal Glauber approximation [73], and the difference is known as Gribov's inelastic corrections [33]. The Glauber's cross section can be corrected by replacing the nuclear thickness function by a reduced one, $T(b)\Rightarrow\widetilde{T}(b)<T(b)$, which is related to the reduced gluon density in the nucleus,

$$\frac{G_A(x,b)}{G_N(x,b)}=\frac{\widetilde{T}(b)}{T(b)}. \tag{117}$$

Thus, nuclear shadowing for soft gluons can be evaluated comparing the total cross section (116) with the modified Glauber approximation,

$$\sigma_{tot}^{hA}=2\int d^2b\left[1-\exp\left(-\frac{1}{2}\sigma_{tot}^{hN}\widetilde{T}(b)\right)\right]. \tag{118}$$

Expanding both expressions in small parameters $\Delta\sigma\,T$ and $\sigma_v\,\Delta T$, where $\Delta T(b)=T(b)-\widetilde{T}(b)$, (they are indeed small even for heavy nuclei) we get

$$\Delta T(b)=\frac{w\,(\Delta\sigma)^2}{4\,\sigma_{tot}^{hN}}T^2(b)\left[1-\frac{1}{6}\Delta\sigma\,T(b)+O((\Delta\sigma T)^2)\right]. \tag{119}$$

We left here only the leading terms and omitted for the sake of simplicity the terms containing higher powers of w.

According to relation (A10) $w\,(\Delta\sigma)^2/16\pi$ is the forward cross section of diffractive gluon radiation which corresponds to the triple-Pomeron part of the diffraction cross section $h\,N\to X\,N$. Therefore, the correction (119) to the nuclear thickness function can be expressed in terms of the effective cross section,

$$\sigma_{eff}=\frac{w\,(\Delta\sigma)^2}{\sigma_{tot}^{hN}}=16\pi A_{3P}(hN\to XN)\ln\left(\frac{M_{max}^2}{M_{min}^2}\right), \tag{120}$$

where $M_{max}^2\approx 2\sqrt{3}\,s/(m_N R_A)$ is the upper cutoff for the diffractive mass spectrum imposed by the the nuclear form factor. The bottom cut off depends on M^2 dependence for the triple-Pomeron diffraction at small masses which is poorly known. At high energies under consideration this uncertainty related to the choice of M_{min}^2 is quite small. We fix $M_{min}=2$ GeV.

Within an approximate Regge factorization scheme $A_{3P}(hN\to XN)$ defined in Eq. (86) is an universal constant [see, however, Eq. (87)]. Therefore, the driving term in Eq. (119) and gluon shadowing are independent of our choice for hadron h, a result which could be expected.

Data on diffractive reaction $pp\to pX$ fix the triple-Pomeron coupling (e.g., see in [46,61,65]) with much better certainty than for other reactions (including data for diffractive DIS). The value of A_{3P} varies from 0.075 GeV^{-2} at medium high energies to 0.025 GeV^{-2} at Tevatron energy [see Eq. (87)]. Correspondingly, the effective cross section for $A\approx 200$ ranges as $\sigma_{eff}\approx 3.5$–5.5 mb. This is an order of magnitude smaller than the value used in [30] at high Q^2. It is very improbable that σ_{eff} can grow (so much) with Q^2.

It is silently assumed in Eq. (116) that the energy is sufficiently high to freeze the fluctuations, i.e., there is no mixing between the Fock components during propagation through the nucleus. If, however, the energy is not high, or the effective mass of the excitation is too large, one should take care of interferences and represent Eqs. (117),(119) in the form (compare to [69,70])

$$\begin{aligned}\frac{G_A(x)}{A\,G_N(x)}=1-8\pi A_{3P}(pp\to pX)&\\ \times\mathrm{Re}\int d^2b\int_{M_{min}^2}^{\infty}\frac{dM_X^2}{M_X^2}\int_{-\infty}^{\infty}dz_1&\\ \times\int_{-\infty}^{\infty}dz_2\,\Theta(z_2-z_1)\times\rho_A(b,z_1)\,\rho_A(b,z_2)&\\ \times\exp[-i\,q_L\,(z_2-z_1)]&\\ \times\exp\left[-\frac{1}{2}\sigma_{abs}\int_{z_1}^{z_2}dz\,\rho_A(b,z)\right],&\end{aligned} \tag{121}$$

where $\sigma_{abs}=\Delta\sigma$, and we exponentiated the expression in square brackets in the RHS of Eq. (117).

The important difference between Eq. (121) and the usual expression [69,70] for inelastic corrections is absence of absorption for the initial ($z<z_1$) and final ($z>z_2$) protons in Eq. (121). This is a natural result, since proton absorption (mostly of eikonal type) has no relevance to gluon shadowing.

Absorption $\sigma_{abs}=\Delta\sigma$ in intermediate state ($z_1>z>z_2$) is much smaller than σ_{tot}^{NN} and is related to the amplitude of diffractive gluon radiation [see (A10)]. One can estimate σ_{abs} assuming Regge factorization. In this case σ_{eff} is universal and can be applied even to a quark, i.e., $h=q$. This makes sense in our model due to the short range nature of the nonperturbative gluon interactions, demanding Eq. (121) to reproduce correctly the ''frozen'' limit of $q_L\to 0$. This needs $\sigma_{abs}=\sigma_{eff}$, as was actually guessed in [30].

However, the discussion following Eq. (42) shows that after it is averaged over the quark-gluon separation the absorptive cross section gains an extra factor, $\sigma_{abs}=1.5\,\sigma_{eff}$.

We performed numerical estimates for $A=200$, 64 and 12 assuming a constant nuclear density $\rho_A(r)=\rho_0\,\Theta(R_A-r)$ with $\rho_0=0.157$ fm^{-3} and $R_A=1.15\,A^{1/3}$ fm. In this case integration in Eq. (121) can be performed analytically and the result reads

$$\begin{aligned}\frac{G_A(x)}{A\,G_N(x)}=1-\frac{1}{3\,\upsilon^3\ln(M_{max}^2/M_{min}^2)}&\\ \times\left\{\left[3-\frac{3}{2}\upsilon^2+\upsilon^3-3\,(1+\upsilon)\,e^{-\upsilon}\right]\right.&\\ \times\left[\ln\left(\frac{s}{m_N R_A\,(M_{min}^2-m_N^2)}\right)-\gamma\right]&\\ +\left[3-\frac{3}{2}\upsilon^2+\upsilon^3\right][\,\gamma+\ln\upsilon-Ei(-\upsilon)]&\\ \left.+\left[\frac{3}{2}\upsilon^2-\frac{11}{2}+\left(\frac{11}{2}+\frac{5}{2}\upsilon-\upsilon^2\right)e^{-\upsilon}\right]\right\},&\end{aligned} \tag{122}$$

where $\upsilon=\frac{3}{2}\,\sigma_{eff}\,\rho_0\,R_A$, $\gamma=0.5772$ is the Euler constant, and $Ei(z)$ is the integral exponential function. The value of x can be evaluated as $x=4\,\langle k^2\rangle/s$, where $\langle k^2\rangle\sim 1/b_0^2$ is the mean transverse momentum squared in the quark-gluon system.

The results of numerical calculations with Eq. (122) for gluon shadowing are depicted in Fig. 6 by thin solid curves for lead, copper and carbon (from bottom to top) as function of x. Shadowing for soft gluons turns out to be much weaker than predicted in [30,31] for high Q^2. This contradicts the natural expectation that the softer gluons are, the stronger shadowing should be.

(ii) The Green function formalism. One can also use the Green function formalism to calculate nuclear shadowing for soft gluon radiation. It provides a better treatment of multiple interactions and phase shifts in intermediate state. In contrast to the above approach which uses a constant average value for σ_{eff}, in the Green function formalism the absorption

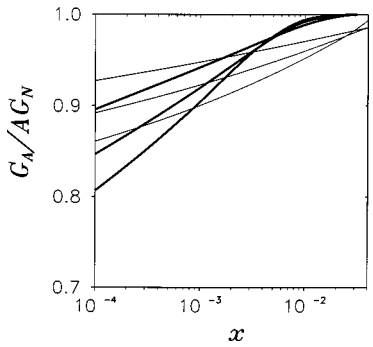

FIG. 6. The same as in Fig. 5, but for soft gluons. The thin curves are obtained with Eq. (122) using data for the triple-Pomeron contribution to diffraction $pp \to pX$. The thick curves are predicted using the Green function method.

cross section as well as the phase shift are functions of longitudinal coordinate. This is also a parameter-free description, all the unknowns have already been fixed by comparison with data.

As usual, we treat shadowing for soft gluons as a contribution of the gluonic Fock component to shadowing of the projectile-nucleus total cross section. One can use as a soft projectile a real photon, a meson, even a single quark. Indeed, the mean quark-gluon separation $1/b_0 \approx 0.3$ fm is much smaller that the quark-antiquark separation in a light meson or a $\overline{qq}$ fluctuation of a photon. For this reason one can neglect in Eq. (49) the interference between the amplitudes of gluon radiation by the q and $\overline{q}$. Since the gluon contribution to the cross section corresponds to the difference between total cross sections for $|\overline{qq}G\rangle$ and $|\overline{qq}\rangle$ components, the quark spectator cancels out and the radiation cross section is controlled by the quark-gluon wave function and color octet (GG) dipole cross section.

Thus, the contribution to the total hadron-nucleus cross section which comes from gluon radiation has the form

$$\sigma_G^{hA} = \int_x^1 \frac{d\,\alpha_G}{\alpha_G} \int d^2b\, P(\alpha_G, \vec{b}), \tag{123}$$

where

$$P(\alpha_G, \vec{b}) = \int_{-\infty}^{\infty} dz\, \rho_A(b,z) \int d^2r\, |\Psi_{qG}(\vec{r}, \alpha_G)|^2\, \sigma_{GG}(r,s)$$
$$-\frac{1}{2}\mathrm{Re}\int_{-\infty}^{\infty} dz_1\, dz_2\, \Theta(z_2 - z_1)$$
$$\times \rho_A(b,z_1)\, \rho_A(b,z_2) \int d^2r_1\, d^2r_2$$
$$\times \Psi^*_{qG}(\vec{r}_2, \alpha_G) \sigma_{GG}(r_2,s)\, G_{GG}(\vec{r}_2, z_2; \vec{r}_1, z_1)$$
$$\times \sigma_{GG}(r_1,s)\, \Psi_{qG}(\vec{r}_1, \alpha_G). \tag{124}$$

Here the energy and Bjorken x are related as $s = 2m_N\nu = 4b_0^2/x$. The explicit solution for the Green function $G_{GG}(\vec{r}_2, z_2; \vec{r}_1, z_1)$ in the case of $\sigma_{GG}(r,s) = C_{GG}(s)\, r^2$ and a constant nuclear density is given by Eq. (65). Note that the r^2 approximation for the dipole cross section is justified by the small value of $\langle r^2 \rangle = 1/b_0^2 \approx 0.1\ \mathrm{fm}^2$.

Integrations in Eq. (124) can be performed analytically,

$$P(\alpha_G, \vec{b}) = \frac{4\,\alpha_G}{3\,\pi}\mathrm{Re}\ln(W), \tag{125}$$

where

$$W = ch(\Omega\,\overline{\Delta z}) + \frac{A^2 + b_0^2}{2\,A\,b_0^2} sh(\Omega\,\overline{\Delta z}), \tag{126}$$

$$\overline{\Delta z} = 2\,\sqrt{R_A^2 - b^2}. \tag{127}$$

We use here the same notations as in Eqs. (109)–(110).

The results of calculations are depicted in Fig. 6 by thick curves for lead, copper and carbon (from bottom to top). They demonstrate about the same magnitude of shadowing as was calculated above using hadronic basis. However, the onset of shadowing is delayed down to $x < 0.01$. We believe that this result is trustable since the Green function approach treats phase shifts and attenuation in nuclear matter more consistently.

Comparing predicted shadowing for soft gluons in Fig. 6 and one at $Q^2 = 4$ GeV in Fig. 5 we arrive at a surprising conclusion that shadowing is independent of scale. A small difference is within the accuracy of calculations. This is a nontrivial result since calculations were done using very different approximations. Shadowing of hard gluons was estimated assuming that the $\overline{qq}$ pair is squeezed to a size $\sim 1/Q$ much smaller than the transverse separation between the gluon and the $\overline{qq}$. On the contrary, radiation of soft gluons is dominated by configurations with a distant q and $\overline{q}$ surrounded by small gluon clouds. The fact that shadowing appears to be the same is a result of existence of the semihard scale b_0^2 (which should be compared with $Q_{eff}^2 < Q^2/4$). At larger virtualities shadowing decreases as one can see from comparison of $Q^2 = 4\ \mathrm{GeV}^2$ with $16\ \mathrm{GeV}^2$ in Fig. 5.

C. Nonperturbative effects in the transverse momentum distribution of gluon bremsstrahlung

As soon as the strength of the nonperturbative quark-gluon interaction is fixed, we are in a position to calculate the cross section of gluon bremsstrahlung for a high energy quark interacting with a nucleon or a nuclear target and to compare the results with the perturbative QCD calculations [36].

1. Nucleon target

The transverse momentum distribution of soft gluons $(\alpha_G \ll 1)$ reads [36]

$$\frac{d\sigma}{d(\ln\alpha_G)\,d^2k_T} = \frac{1}{2\,(2\pi)^2}\int d^2r_1\,d^2r_2\,\overline{\Psi^\dagger_{qG}(\vec{r}_1,\alpha_G)\,\Psi_{qG}(\vec{r}_2,\alpha_G)} \times \exp[i\,\vec{k}_T(\vec{r}_1-\vec{r}_2)][\sigma_{GG}(r_1)+\sigma_{GG}(r_2) - \sigma_{GG}(\vec{r}_1-\vec{r}_2)]. \quad (128)$$

Here the overline means that we sum over all possible polarizations of the radiated gluon and recoil quark and average over the polarization of the initial quark. In our model for the quark-gluon distribution function including nonperturbative effects we get

$$\overline{\Psi^\dagger_{qG}(\vec{r}_1,\alpha_G)\,\Psi_{qG}(\vec{r}_2,\alpha_G)} = \frac{4\,\alpha_s}{3\pi^2 r_1^2 r_2^2}\vec{r}_1\cdot\vec{r}_2\exp\left[-\frac{b_0^2}{2}(r_1^2+r_2^2)\right]. \quad (129)$$

The cross section $\sigma_{GG}(r)$ in Eq. (128) has the form (104).

We performed calculations for the transverse momentum distribution of gluons for two parametrizations of the dipole cross section, (I) one which is given by Eq. (30) which is constant at $\rho^2 \gg \rho_0^2$. For the sake of convenience we change the notation here, $s^2=2/\rho_0^2=0.125\,\mathrm{GeV}^{-2}$; (II) the dipole approximation (5) with $C=\sigma_0 s^2/2$. Only this parametrization is used for nuclear targets because it allows to perform integrations analytically (of course one can do numerical calculation for any shape of the cross section).

Correspondingly, we obtain for the differential radiation cross section,

$$\frac{d\sigma_I^N}{d(\ln\alpha_G)\,d^2k_T} = \frac{3\,\alpha_s\,\sigma_0}{\pi^2}F(k_T^2,b_0^2,s^2), \quad (130)$$

where

$$F(k_T^2,b_0^2,s^2) = \frac{1}{2\,k_T^2}\Omega_1\,(\Omega_1-2\,\Omega_2)+\frac{1}{4\,s^2}\left[Ei\left(\frac{k_T^2}{2\,s^2}\right) - 2\,Ei\left(\frac{k_T^2}{2\,s^2}x_1\right)+Ei\left(\frac{k_T^2}{2\,s^2}x_2\right)\right] \quad (131)$$

$$\Omega_1 = 1-\exp\left(-\frac{k_T^2}{2\,b_0^2}\right);$$

$$\Omega_2 = 1-\exp\left[-\frac{k_T^2}{2\,(b_0^2+s^2)}\right];$$

$$x_1=\frac{b_0^2}{b_0^2+s^2};\quad x_2=\frac{b_0^2}{b_0^2+2\,s^2};$$

and $\mathrm{Ei}(z)$ is the exponential integral function.

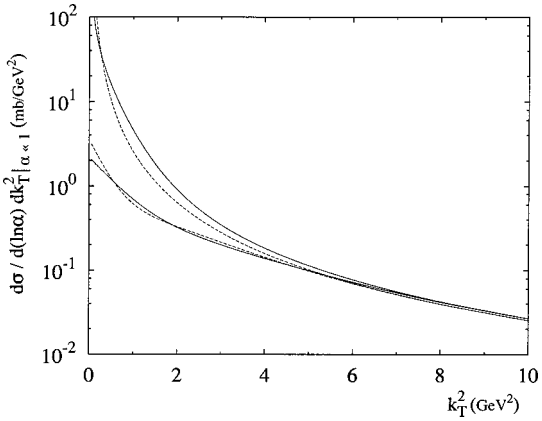

FIG. 7. Transverse momentum distribution for gluon bremsstrahlung by a quark scattering on a nucleon target. The solid and dashed curves correspond to parametrizations I and II for the dipole cross section, respectively. The upper curves show the results of the perturbative QCD predictions [36]; the bottom curves correspond to the full calculation including the nonperturbative interaction of the radiated gluon.

In the case of parameterization II it is convenient to represent the dipole cross section in the form

$$\sigma_{qq}^{-}(r) = \sigma_0\,s^2\frac{d}{d\,s^2}\left[1-\exp\left(-\frac{1}{2}s^2\,r^2\right)\right]_{s^2=0}. \quad (132)$$

Then the differential cross section reads

$$\frac{d\sigma_{II}^N}{d(\ln\alpha_G)\,d^2k_T} = \frac{3\,\alpha_s\sigma_0\,s^2}{\pi^2}F_1(k_T^2,b_0^2,s^2), \quad (133)$$

where

$$F_1(k_T^2,b_0^2,s^2) = \frac{d}{d\,s^2}F(k_T^2,b_0^2,s^2)|_{s^2=0} = \Lambda_1^2-\Lambda_1\,\Lambda_2+\frac{1}{2}\Lambda_2^2; \quad (134)$$

$$\Lambda_1=\frac{1}{k_T^2}\Omega_1=\frac{1}{k_T^2}\left[1-\exp\left(-\frac{k_T^2}{2\,b_0^2}\right)\right];$$

$$\Lambda_2=\frac{1}{k_T^2}\exp\left(-\frac{k_T^2}{2\,b_0^2}\right).$$

The results of calculations for variants I and II are depicted in Fig. 7 by solid and dashed curves, respectively. The two upper curves correspond to perturbative calculations, while the two bottom ones include the nonperturbative effects. The strong interaction between gluon and quark leads to a substantial decrease in the mean transverse size of the quark-gluon fluctuation. Therefore, the mean transverse momentum of the radiated gluons increases. The nonperturbative interaction has especially strong effect at small transverse momentum k_T, where the radiation cross section turns

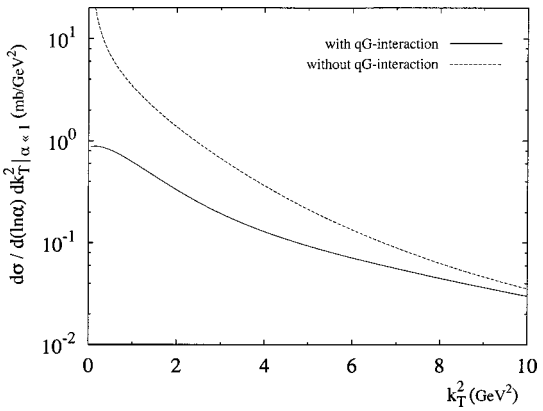

FIG. 8. The differential cross ection per bound nucleon of soft gluon bremsstrahlung in quark-copper collisiions. The solid and dashed cruves correspond to calculations with and without the nonperturbative effects, respectively.

out to be suppressed by almost two orders of magnitude compared to the perturbative QCD expectations.

Note that intensive gluon radiation originating from multiple nucleon interactions in relativistic heavy ion collisions is found [78,79] to be an important alternative source for suppression of charmonium production rate and is able to explain the corresponding data from the NA50 experiment at CERN Super Proton Synchrotron (SPS). The found strong suppression of gluon bremsstrahlung by the nonperturbative interaction relevant only to small $\alpha \ll 1$. However, it may substantially reduce the influence of prompt gluons on charmonium production if is important at large α as well. This is to be checked.

2. Nuclear targets

In the case of nuclear targets Eq. (128) holds, but $\sigma_{GG}(r)$ has the form

$$\sigma^A_{GG}(r) = 2 \int d^2B \left\{ 1 - \exp\left[-\frac{9}{8} \sigma^-_{qq}(r)\, T(B) \right] \right\}. \tag{135}$$

Our calculations for gluon radiation in the interaction of a quark with a nuclear target are performed only in the parametrization II for the sake of simplicity. For heavy nuclei this approximation can be quite good due to a strong color filtering effect which diminishes the contribution from large size dipoles. The transverse momentum distribution has the form

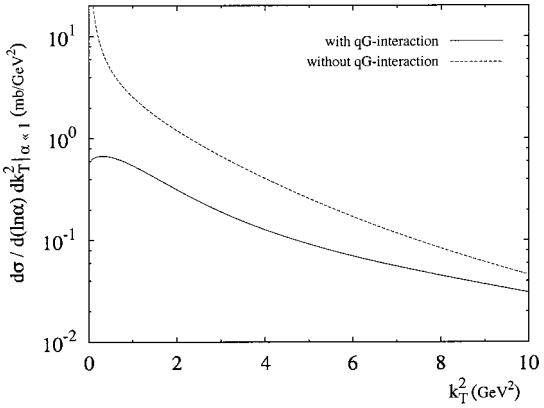

FIG. 9. The same as in Fig. 8, but for a lead target.

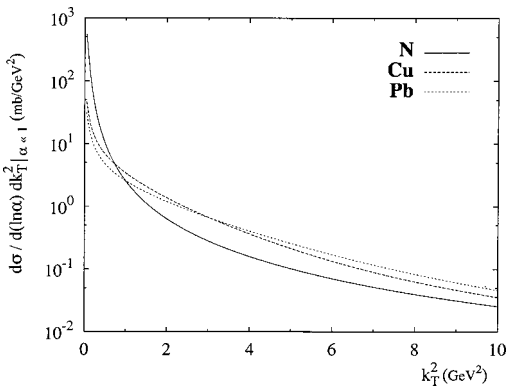

FIG. 10. Comparison of the cross sections of gluon radiation per nucleon in the perturbative QCD limit for collisions of a quark with a nucleon (solid curve), copper (dashed curve) and lead (dotted curve) versus the transverse momentum squared of the gluon.

$$\frac{d\sigma^A_{II}}{d(\ln \alpha_G)\, d^2k_T} = \frac{8\alpha_s}{3\pi^2} \int d^2B\, F(k_T^2, b_0^2, S^2(B)), \tag{136}$$

where

$$S^2(B) = \frac{9}{8} \sigma_0\, s^2\, T(B). \tag{137}$$

For numerical calculations we use the approximation of constant nuclear density, $\rho_A(r) = 3A/(4\pi R_A^3)\, \Theta(R_A - r)$. The results for the radiation cross section per bound nucleon with (solid curve) and without (dashed) the nonperturbative effects are compared in Figs. 8 and 9 for copper and lead targets, respectively. Obviously the nonperturbative interaction generates very large nuclear effects.

The nuclear effects are emphasized by a direct comparison in Figs. 10 and 11 for different targets, a nucleon, copper and lead, including and excluding the nonperturbative interaction respectively. We see that the difference between a free and a bound nucleon at small k_T is substantially reduced by the nonperturbative interaction. Indeed, the interaction

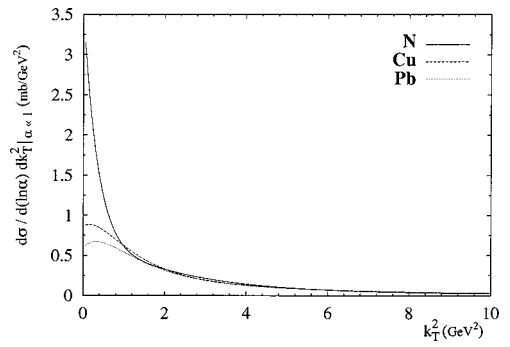

FIG. 11. The same as in Fig. 10, but the nonperturbative interaction of gluons is included.

squeezes the quark-gluon fluctuation and reduces the nuclear effects. Besides, the region of antishadowing is pushed to larger values of k_T.

This manifestation of the nonperturbative interaction implies that gluon saturation which is an ultimate form of shadowing should happen with a smaller gluon density compared to the expectations [24,25] based on perturbative calculations. On the other hand, the saturation region spreads up to higher values of k_T.

IV. SUMMARY AND OUTLOOK

We explicitly introduced a nonperturbative interaction between partons into the evolution equation for the Green function of a system of quarks and gluons. The shape of the $\bar{q}q$ potential is chosen to reproduce the light cone wave function of mesons. The magnitude of the potential is adjusted to reproduce data for photoapsorptive cross sections on nucleons and nuclei and data on diffractive dissociation of photons into $\bar{q}q$ pairs.

Based on theoretical arguments and experimental facts we expect a much stronger interaction for a quark-gluon pair than for a quark-antiquark pair. Indeed, data on diffractive dissociation of hadrons and photons into high mass states show that the cross section is amazingly small, what is usually phrased as evidence that the triple-Pomeron coupling is small. We have performed calculations for diffractive gluon radiation (responsible for the production of high mass excitations) including the nonperturbative effects, and fixed the strength of the quark-gluon potential. We found a very simple and intuitive way to get the same results as direct calculations of Feynman diagrams. Both approaches lead to the same diffractive cross section which in the limit of perturbative QCD coincides with the result of a recent calculation [19] for the process $\gamma^* N \to \bar{q}qGN$. We conclude that the previous analogous calculations [18] are incorrect.

We adjusted the quark-gluon potential to data for the diffractive reaction $pp \to Xp$ which have the best accuracy and cover the largest range of energies and masses. We predicted the single diffractive cross sections for pions, kaons and photons and find a substantial violation of Regge factorization.

We calculated nuclear shadowing for longitudinally polarized photons which are known to serve as a sensitive probe for the gluon distribution, using the Green function technique developed in [12] describing the evolution of a $\bar{q}qG$ system propagating through nuclear matter. The evolution equation includes the phase shift which depends on the effective mass of the fluctuation, nuclear attenuation which depends on the transverse separation and energy, and the distribution over transverse separation and longitudinal momenta of the partons which is essentially affected by the nonperturbative interaction of the gluon. The latter substantially reduces the effect of nuclear shadowing of gluons. We have found an x dependence for gluons which is quite different from that for quarks. These differences are far beyond the simple Casimir factor 9/4.

Nuclear shadowing for soft gluons is essentially controlled by the nonperturbative effects. It turns out to be rather weak similar to what is found at $Q^2 \sim 4\ \mathrm{GeV}^2$. Such a scale invariance at low and medium high virtualities is a consequence of the strong nonperturbative interaction of gluons which introduces a semihard scale $\sim 4\, b_0^2 = 1.7\ \mathrm{GeV}^2$.

The nonperturbative interaction changes dramatically the transverse momentum distribution of gluon bremsstrahlung by a high energy quark interacting with a nucleon or a nucleus. The gluon radiation cross section at small k_T turns out to be suppressed by nearly two orders of magnitude compared to the expectations from perturbative QCD [50,36]. Although these results concern the gluons radiated with $\alpha_G \to 0$, it might also suppress gluon bremsstrahlung at larger α_G which is predicted [78] to contribute to the break up of charmonia produced in relativistic heavy ion collisions.

This effect is especially strong for nuclear targets where the nonperturbative interaction of radiated gluons creates a forward minimum in the transverse momentum distribution. This suppression is an additional contribution to nuclear shadowing calculated perturbatively in [50,36] which also leads to a suppression of small transverse momenta. The results of our calculations presented in Figs. 8, 9 include both phenomena.

Nuclear shadowing for small transverse momenta of the radiated gluons is the same effect as the saturation of parton densities at small x in nuclei as seen in the infinite momentum frame of the nucleus. This phenomenon is expected to be extremely important for the problem of quark-gluon plasma formation in relativistic heavy ion collisions. On the one hand, a growth of the mean transverse momentum of radiated gluons increases the produced transverse energy, on the other hand, it leads to a higher probability for such gluons to escape the interaction region without collisions, i.e., the gluon gas may not reach equilibrium [80].

ACKNOWLEDGMENTS

We are grateful to Yuri Ivanov and Jörg Raufeisen for their constant assistance in numerical calculations and to Jörg Hüfner, Mikkel Johnson, Andrei Leonidov and Hans-Jürgen Pirner for useful discussions. A substantial part of this work was done when A.V.T. was employed by the Institut für Theoretische Physik der Universität, Heidelberg and was supported by the Gesellschaft für Schwerionenforschung, GSI, grant HD HÜF T.

APPENDIX A: DIFFRACTION

1. General consideration

In this section we present a general analysis of diffraction based on the eigenstate decomposition.

The off-diagonal diffractive scattering is a direct consequence of the fact that the interacting particles (hadrons, photon) are not eigenstates of the interaction Hamiltonian [81,82]. They can be decomposed in a complete set of such eigenstates $|k\rangle$ [74,83],

$$|h\rangle = \sum_k C_k^h |k\rangle, \tag{A1}$$

where C_k^h are the amplitudes for the decomposition which obey the orthogonality conditions

$$\sum_k (C_k^{h'})^\dagger C_k^h = \delta_{h\,h'};$$

$$\sum_h (C_l^h)^\dagger C_k^h = \delta_{lk}. \tag{A2}$$

We denote by $f_k = i\,\sigma_k/2$ the eigenvalues of the elastic amplitude operator $\hat{f}$. We assume that the amplitude is integrated over impact parameter, i.e., that the forward scattering elastic amplitude is normalized as $|f_k|^2 = 4\,\pi\, d\sigma_k/dt|_{t=0}$. We can then express the hadronic amplitudes, the elastic $f_{el}(hh)$ and off diagonal diffractive $f_{dd}(hh')$ amplitudes as

$$f_{el}(hh) = 2i \sum_k |C_k^h|^2\, \sigma_k \equiv 2i\,\langle\sigma\rangle; \tag{A3}$$

$$f_{dd}(hh') = 2i \sum_k (C_k^{h'})^\dagger C_k^h\, \sigma_k. \tag{A4}$$

Note that if all the eigen amplitudes are equal the diffractive amplitude (A4) vanishes due to the orthogonality relation (A2). The physical reason is obvious. If all the f_k are identical the interaction does not affect the coherence between the different eigen components $|k\rangle$ of the projectile hadron $|h\rangle$. Therefore, off diagonal transitions are possible only due to differences between the f_k's. For instance, in the two channel case,

$$f_{dd}(hh') = 2i(C_2^h)^\dagger C_1^h(\sigma_1 - \sigma_2). \tag{A5}$$

If one sums over all final states in the diffractive cross section one can use the completeness condition (A2). Excluding the elastic channels one gets [74,83,5]

$$16\pi \left.\frac{d\sigma_{dd}^h}{dt}\right|_{t=0} = \sum_i |C_i^h|^2 \sigma_i^2 - \left(\sum_i |C_i^h|^2 \sigma_i\right)^2 \equiv \langle\sigma_i^2\rangle - \langle\sigma\rangle^2. \tag{A6}$$

This formula is valid only for the total (forward) diffractive cross section and cannot be used for exclusive channels.

2. Diffractive excitation of a quark, $q \to qG$

In this case we can restrict ourselves to the first two Fock components of the quark, a bare quark $|q\rangle$ and $|qG\rangle$. Therefore, we can use Eq. (A5). Thus, we arrive at the following expression for the forward amplitude of diffractive dissociation into a qG pair with transverse separation $\vec{\rho}$:

$$f_{dd}(q \to qG)|_{q_T=0} = i\,\Psi_{qG}(\alpha,\vec{\rho})\,[\sigma_{qG}(\rho) - \sigma_q]. \tag{A7}$$

Both cross sections, σ_{qG} and σ_q are infrared divergent, but this divergence is obviously the same and cancels in Eq. (A7).

To regulate the divergence we can introduce a small gluon mass m_G, which will not enter the final result, and impose that for separations $r \gg 1/m_G$ the dipole cross section is given by the additive quark limit, $\sigma_{\bar{q}q}(r \gg 1/m_G) = 2\,\sigma_q$. To find the convergent part of $\sigma_{qG}(\rho) - \sigma_q$ we can make use of Eq. (47). Let us choose in Eq. (47) $r_1 \ll 1/m_G$ and $r_2 \gg 1/m_G$. Then the LHS of Eq. (47) saturates at $\sigma_q + \sigma_{qG}(r_1)$. Here $\sigma_{qG}(r_1)$ is different from $\sigma_{\bar{q}}$ due to the color dipole moment of the qG system, i.e., due to $r_1 \neq 0$. Then Eq. (47) is modified to

$$\sigma_q + \sigma_{qG}(r_1) = \frac{9}{8}\{\sigma_{\bar{q}q}(r_1) + 2\,\sigma_q\} - \frac{2}{8}\sigma_q. \tag{A8}$$

From this relation we obtain the combination of cross sections at the RHS of Eq. (A7) which takes the form

$$f_{dd}(q \to qG)|_{q_T=0} = i\,\Psi_{qG}(\alpha,\vec{\rho})\,\frac{9}{8}\,\sigma_{\bar{q}q}(\rho). \tag{A9}$$

Thus, we derived Eq. (60) in a simple and intuitive way. A more formal derivation based on direct calculation of Feynman diagrams is presented in Appendix B.1.

3. Diffractive gluon radiation by a $\bar{q}q$ pair

The diffractive amplitude of gluon radiation by a $\bar{q}q$ pair, $\bar{q}q \to \bar{q}qG$, can be easily derived in this approach. We restrict ourselves to two Fock components $|\bar{q}q\rangle$ and $|\bar{q}qG\rangle$. Then the distribution amplitudes C_k^h get the meaning of distribution functions for these Fock states, namely $\Psi_{\bar{q}q}(\vec{r}_1 - \vec{r}_2, \alpha)$ and $\Psi_{G\bar{q}q}(\vec{\rho}_1, \vec{\rho}_2, \alpha, \alpha_G)$, where the transverse coordinates are defined in Eq. (82). Summation over k in Eqs. (A1)–(A4) now means integration over the transverse separations and summation over the Fock components. According to Eqs. (A4) and (A5) the diffractive amplitude $f_{dd}(\bar{q}q \to \bar{q}qG)$ reads,

$$f_{dd}(\bar{q}q \to \bar{q}qG) = 2\int d^2\rho_1\, d^2\rho_2\, \Psi_{\bar{q}qG}^*(\vec{\rho}_1, \vec{\rho}_2, \alpha, \alpha_G) \times [\sigma_{G\bar{q}q}(\vec{\rho}_1, \vec{\rho}_2) - \sigma_{\bar{q}q}(\vec{\rho}_1 - \vec{\rho}_2)]. \tag{A10}$$

Here we make use of the obvious relation $C^{\bar{q}q}(\vec{r}) = \delta(\vec{r})$. The total cross sections for the two Fock components $\bar{q}q$ and $G\bar{q}q$ are introduced in Eqs. (9) and (47).

The distribution amplitude for the $G\bar{q}q$ fluctuation in the limit of $\alpha_G \to 0$ is easily guessed. Indeed, in this limit the impact parameters of the q and $\bar{q}$ are not affected by gluon radiation. Therefore, the $\Psi_{\bar{q}qG}^*$ should be a product of the $\bar{q}q$ distribution function in the projectile hadron (photon) times the sum of the gluon distribution amplitudes corresponding to radiation of the gluon by q or $\bar{q}$,

$$\Psi^{-}_{\bar{q}qG}(\vec{\rho}_1,\vec{\rho}_2,\alpha,\alpha_G) = \Psi^{-}_{\bar{q}q}(\vec{\rho}_1-\vec{\rho}_2,\alpha)\left[\Psi_{qG}\left(\vec{\rho}_1,\frac{\alpha_G}{\alpha}\right) - \Psi^{-}_{qG}\left(\vec{\rho}_2,\frac{\alpha_G}{1-\alpha}\right)\right], \tag{A11}$$

where $\Psi^{-}_{\bar{q}q}$ and Ψ_{qG} are defined in Eqs. (18),(19) and in (56) respectively. Thus, we have arrived at Eq. (83). A more formal derivation based on the calculation of Feynman graphs is presented in the next Appendix.

After integration over $(\vec{\rho}_1+\vec{\rho}_2)$ in Eq. (A10) the amplitude of diffractive gluon radiation turns out to be proportional to the difference $\Delta\sigma(\vec{\rho}_1-\vec{\rho}_2)$ between the cross sections of the colorless systems $G\bar{q}q$ and $\bar{q}q$. This is a straightforward consequence of the general property of off-diagonal diffractive amplitudes given in Eq. (A5).

These conclusions are also valid for diffractive gluon radiation by a photon $\gamma N\to\bar{q}qGN$. At first glance presence of a third channel, the photon, may change the situation and gluon radiation amplitude may not be proportional to $\Delta\sigma$. This is not true, however, since the relative weights of the $\bar{q}q$ and $\bar{q}qG$ components of the photon are the same as above as soon as they are generated perturbatively.

In the limit of purely perturbative interactions the same result as our Eq. (83) was obtained recently in [19] [Eq. (3.4)]. However, the cross section for diffractive gluon radiation derived earlier in [18] [Eq. (60)] is not proportional to $(\Delta\sigma)^2$, but contains a linear term. We think that this is a consequence of improper application of relation (A6) to an exclusive channel.

4. Diffractive electromagnetic radiation

The forward amplitude for photon (real or virtual) radiation by a quark is similar to that for gluon radiation (A7), except that the photon does not interact strongly and one has to replace σ_{qG} by σ_q,

$$f_{dd}(q\to q\gamma^*)|_{q_T=0} = i\,\Psi_{q\gamma^*}(\alpha,\vec{\rho})\,[\sigma_q-\sigma_q]=0. \tag{A12}$$

Thus, in order to radiate a photon the quark has to get a kick from the target, no radiation happens if the momentum transfer to the target is zero.

This conclusion is different from the expectation for diffractive Drell-Yan pair production of [20]. The latter was based on the conventional formula (A10) which cannot be used for an exclusive channel (as well as for gluon radiation). Therefore, the diffractive Drell-Yan cross section should be much smaller than estimated in [20].

Nevertheless, a hadron as a whole can radiate diffractively a photon without momentum transfer as two of its quarks can participate in diffractive scattering, each of them may getting a momentum transfer, while the total momentum transfer is zero.

APPENDIX B: DIFFRACTION: FEYNMAN DIAGRAMS

1. $qN\to qGN$

For the example of diffractive excitation of a quark,

$$qN\to qGN, \tag{B1}$$

we demonstrate in the following the techniques and approximations we use for the calculation of more complicated diffractive processes.

We use the following notations for the kinematics of Eq. (B1): $\vec{k}_T$ and $\vec{p}_T$ are the transverse momenta of the final gluon and quark respectively; α is the fraction of the initial light-cone momentum carried by the gluon; $\vec{q}_T=\vec{k}_T+\vec{p}_T$ is the total transverse momentum of the final quark and gluon, and $\vec{\kappa}_T=(1-\alpha)\vec{k}_T-\alpha\vec{p}_T$ appears further on, when the transverse separations $\vec{r}_G=\vec{b}+(1-\alpha)\vec{\rho}$ and $\vec{r}_q=\vec{b}+\alpha\vec{\rho}$ are inserted: $\vec{k}_T\cdot\vec{r}_G+\vec{p}_T\cdot\vec{r}_q=(\vec{k}_T+\vec{p}_T)\cdot\vec{b}+((1-\alpha)\vec{k}_T+\alpha\vec{p}_T)\cdot\vec{\rho}$.

We normalize the amplitude of Eq. (B1) according to

$$\frac{d\sigma(qN\to qGN)}{d\ln\alpha d^2\kappa_T d^2q_T} = \frac{1}{3}\sum_{\mu,nu,s}|A_s^{(\mu,\nu)}(\vec{q}_T,\vec{\kappa}_T,\alpha)|^2 = \frac{1}{3}\sum_s \mathrm{Tr}[A_s^\dagger(\vec{q}_T,\vec{\kappa}_T,\alpha)\,A_s(\vec{q}_T,\vec{\kappa}_T,\alpha)], \tag{B2}$$

where

$$A_s^{(\mu,\nu)}=(q^\mu)^\dagger\,\hat{A}_s\,q^\nu, \tag{B3}$$

and $q^{\nu(\mu)}$ are the color spinors of the quark in the initial and final states; s is the color index of the radiated gluon.

We assume that at high energies one can neglect the ratio of the real to imaginary parts of the amplitude for reaction (B1). Then one can apply the generalized optical theorem (*Cutkosky rules* [58]),

$$\hat{A}(a\to b)=\frac{i}{2}\sum_c\,\hat{A}^\dagger(b\to c)\,\hat{A}(a\to c). \tag{B4}$$

Here Σ_c includes not only a sum over intermediate channels, but also an integration over the intermediate particle momenta.

To simplify the problem we switch to the impact parameter representation,

$$\hat{A}(\vec{b},\vec{\rho})=\frac{1}{(2\pi)^2}\int d^2q\,d^2\kappa_T\,\hat{A}(\vec{q}_T,\vec{\kappa}_T) \times\exp(-i\,\vec{q}_T\vec{b}-i\,\vec{\kappa}_T\vec{\rho}). \tag{B5}$$

Since the initial impact parameters are preserved during the interaction we sum only over intermediate channels in this representation.

We use the Born approximation, i.e., the lowest order in α_s, for the sake of clarity, and generalization is straightforward. In this case and for $a=\{qN\}$, $b=\{qGN\}$ only two

intermediate states are possible in Eq. (B4): $c_1=\{q\,N_8^*\}$ and $c_2=\{q\,G\,N_8^*\}$, where $N_8^*\equiv|3q\rangle_8$ is the octet color state of the $3q$ system produced when the nucleon absorbs the exchanged gluon.

One should sum in Eq. (B4) over all excitations f of the N_8^*,

$$\hat{A}_s(qN\to qGN)=\sum_f\Big[\hat{A}_s^\dagger(qGN\to qN_8^*)\,\hat{A}(qN\to qN_8^*)+\sum_{s'}\hat{A}_{s's}^\dagger(qGN\to qGN_8^*)\times\hat{A}_{s'}(qN\to qGN_8^*)\Big]. \tag{B6}$$

Here s' is the color index of the gluon in the intermediate state.

We skip the simple but lengthy details of calculation of the amplitudes on the RHS of Eq. (B6) and present only the results:

$$\hat{A}(qN\to qN_8^*)=\tau_r\langle f|\hat{\gamma}_r(\vec{b}_1)|i\rangle; \tag{B7}$$

$$\hat{A}_s'(qN\to qGN_8^*)=[\tau_{s'}\,\tau_r\langle f|\hat{\gamma}_r(\vec{b}_1)|i\rangle-\tau_r\,\tau_{s'}\langle f|\hat{\gamma}_r(\vec{b}_2)|i\rangle-i\,f_{s'rp}\tau_p\langle f|\hat{\gamma}_r(\vec{b}_3)|i\rangle]\frac{\sqrt{3}}{2}\Psi_{qG}(\alpha,\vec{\rho}); \tag{B8}$$

$$\hat{A}_s(qGN\to qN_8^*)=[\tau_r\,\tau_s\langle f|\hat{\gamma}_r(\vec{b}_1)|i\rangle-\tau_s\,\tau_r\langle f|\hat{\gamma}_r(\vec{b}_2)|i\rangle-i\,f_{rsp}\tau_p\langle f|\hat{\gamma}_r(\vec{b}_3)|i\rangle]\frac{\sqrt{3}}{2}\Psi_{qG}(\alpha,\vec{\rho}); \tag{B9}$$

$$\hat{A}_{ss'}(qGN\to qGN_8^*)=\delta_{ss'}\tau_r\langle f|\hat{\gamma}_r(\vec{b}_2)|i\rangle+i\,f_{ss'r}\langle f|\hat{\gamma}_r(\vec{b}_3)|i\rangle. \tag{B10}$$

Here $\vec{b}_1=\vec{b}$; $\vec{b}_2=\vec{b}-\alpha\vec{\rho}$ are the impact parameters of the projectile and ejectile quarks in reaction (B1), respectively; $\vec{b}_3=\vec{b}+(1-\alpha)\vec{\rho}$ is the impact parameter of the radiated gluon; $\vec{\rho}$ is the transverse separation inside the qG system, and $\vec{b}$ is the distance from its center of gravity to the nucleon target; $\Psi_{qG}(\alpha,\vec{\rho})$ is the distribution function for the qG pair; $\lambda_r=2\,\tau_r$ are the Gell-Mann matrices; f_{rsp} is the structure constant for the $SU(3)$ group. The matrices $\hat{\gamma}_r(\vec{b}_k)$, $(k=1,2,3)$ are the operators in coordinate and color space for the target quarks,

$$\hat{\gamma}_r(\vec{b}_k)=\sum_{j=1}^{3}\tau_r^{(j)}\,\chi(\vec{b}_k-\vec{s}_i) \tag{B11}$$

$$\chi(\vec{\beta})=\frac{1}{\pi}\int d^2q\,\frac{\alpha_s(q)\exp(i\vec{q}_T\vec{\beta})}{q^2+\Lambda^2}, \tag{B12}$$

where $\vec{s}_i$ is the transverse distance between the jth valence quark of the target nucleon and its center of gravity; the matrices $\tau_r^{(j)}$ act on the color indices of this quark. The matrix elements $\langle f|\hat{\gamma}_r(\vec{b}_k)|i\rangle$ between the initial $i=N$ and final $f=N_8^*$ states are expressed through the wave functions of these states. The effective infrared cutoff Λ in Eq. (B12) does not affect our results, which are infra-red stable due to color screening effects.

Substitution of Eqs. (B7)–(B10) into Eq. (B6) results in

$$\hat{A}_s(qN\to qGN)=\frac{i}{2}\{\tau_s\,\tau_r\,\tau_{r'}|\Phi_{rr'}(\vec{b}_1,\vec{b}_1)-\tau_r\,\tau_s\,\tau_{r'}|\Phi_{rr'}(\vec{b}_2,\vec{b}_1)+i\,f_{rsp}\,\tau_p\,\tau_{r'}|\Phi_{rr'}(\vec{b}_3,\vec{b}_1)+\tau_r\,\tau_s\,\tau_{r'}|\times\Phi_{rr'}(\vec{b}_1,\vec{b}_2)-\tau_s\,\tau_r\,\tau_{r'}|\Phi_{rr'}(\vec{b}_2,\vec{b}_2)-i\,f_{rsp}\,\tau_p\,\tau_{r'}|\Phi_{rr'}(\vec{b}_2,\vec{b}_3)-i\,f_{ss'r}[\tau_{s'}\,\tau_{r'}|\Phi_{rr'}(\vec{b}_1,\vec{b}_3)-\tau_{r'}\,\tau_{s'}|\Phi_{rr'}(\vec{b}_2,\vec{b}_3)-i\,f_{s'r'p}\,\tau_p\,\Phi_{rr'}(\vec{b}_3,\vec{b}_3)]\}\frac{\sqrt{3}}{2}\Psi_{qG}(\alpha,\vec{\rho}), \tag{B13}$$

where

$$\Phi_{rr'}(\vec{b}_k,\vec{b}_l)=\sum_f\langle i|\hat{\gamma}_r(\vec{b}_k)|f\rangle\langle f|\hat{\gamma}_{r'}(\vec{b}_l)|i\rangle. \tag{B14}$$

We sum in Eq. (B13) over all excitations of the two color octet states of the $3q$ system. To have a complete set of states we have to include also color singlet and decuplet $|3q\rangle$ states. As these states cannot be produced via single gluon exchange, they do not contribute and we can simply extend the summation in Eq. (B14) to the complete set of states and get

$$\Phi_{rr'}(\vec{b}_k,\vec{b}_l)=\langle i|\hat{\gamma}_r(\vec{b}_k)\hat{\gamma}_{r'}(\vec{b}_l)|i\rangle. \tag{B15}$$

In the matrix element (B15) we average over color indices

of the valence quarks and their relative coordinates in the target nucleon. To do so one should use the relation

$$\langle \tau_r^{(j)} \cdot \tau_{r'}^{(j')} \rangle_{|3q\rangle_1} = \begin{cases} \frac{1}{6}\,\delta_{rr'} & (j=j'), \\ -\frac{1}{12}\,\delta_{rr'} & (j\neq j'). \end{cases} \tag{B16}$$

Then, Eq. (B15) can be represented as

$$\Phi_{rr'}(\vec{b}_k,\vec{b}_l) = \frac{3}{4}\,\delta_{rr'}\,S(\vec{b}_k,\vec{b}_l), \tag{B17}$$

where $S(\vec{b}_k,\vec{b}_l)$ is a scalar function of two vector variables,

$$S(\vec{b}_k,\vec{b}_l) = \frac{2}{9}\int d\{s\}\left[\sum_{j=1}^{3}\chi(\vec{b}_k-\vec{s}_j)\,\chi(\vec{b}_l-\vec{s}_j) - \frac{1}{2}\sum_{j\neq j'}\chi(\vec{b}_k-\vec{s}_j)\,\chi(\vec{b}_l-\vec{s}_{j'})\right]|\Phi_{3q}(\{s\})|^2. \tag{B18}$$

This function is directly related to the $\bar{q}q$ dipole cross section (5),

$$\sigma_{qq}^{-}(\vec{\rho}_1-\vec{\rho}_2) = \int d^2b\,[S(\vec{b}+\vec{\rho}_1,\vec{b}+\vec{\rho}_1)+S(\vec{b}+\vec{\rho}_2,\vec{b}+\vec{\rho}_2) - 2\,S(\vec{b}+\vec{\rho}_1,\vec{b}+\vec{\rho}_2)]. \tag{B19}$$

According to Eqs. (B17) and (B18) the function $\Phi(\vec{b}_k,\vec{b}_l)$ is symmetric under the replacement $\vec{b}_k \rightleftharpoons \vec{b}_l$. Therefore, the terms proportional to $\Phi(\vec{b}_1,\vec{b}_2)$ and $\Phi(\vec{b}_2,\vec{b}_1)$ in Eq. (B13) cancel, as well as the terms proportional to $\Phi(\vec{b}_1,\vec{b}_3)$ and $\Phi(\vec{b}_3,\vec{b}_1)$. At the same time, the terms proportional to $\Phi(\vec{b}_2,\vec{b}_3)$ and $\Phi(\vec{b}_3,\vec{b}_2)$ add up.

Making use of the relations

$$\tau_r\tau_r = 4/3$$

$$f_{ss'r}\,f_{s'rp} = 3\,\delta_{sp}$$

$$-i\,f_{rsp}\,\tau_p\,\tau_r = \frac{3}{2}\,\tau_s, \tag{B20}$$

we arrive at the final result for the amplitude of diffractive dissociation of a quark ($q\,N\to q\,G\,N$) in impact parameter representation,

$$\hat{A}_s(\vec{b},\vec{\rho},\alpha) = \frac{i\,3\sqrt{3}}{16}\,\tau_s\,\Psi_{qG}(\alpha,\vec{\rho}) \times\left\{\frac{4}{3}[S(\vec{b}_1,\vec{b}_1)-S(\vec{b}_2,\vec{b}_2)] + 3\,[S(\vec{b}_1,\vec{b}_3)-S(\vec{b}_3,\vec{b}_3)]\right\}. \tag{B21}$$

The diffraction amplitude in momentum representation reads

$$\hat{A}_s(\vec{q}_T,\vec{\kappa}_T,\alpha) = \frac{1}{(2\pi)^2}\int d^2b\,d^2\rho\,\hat{A}_s(\vec{b},\vec{\rho},\alpha) \times\exp(i\,\vec{q}_T\vec{b}+i\,\vec{\kappa}_T\vec{\rho}). \tag{B22}$$

Using Eq. (B19) and the above mentioned symmetry of $S(\vec{\rho}_1,\vec{\rho}_2)$ we obtain a very simple expression for the forward ($q_T=0$) diffraction amplitude which is related to the dipole cross section,

$$\hat{A}_s(0,\vec{\kappa}_T,\alpha) = -\frac{i9\sqrt{3}}{32\,(2\pi)^2}\,\tau_s\int d^2\rho\,\Psi_{qG}(\alpha,\vec{\rho}) \times\sigma_{qq}^{-}(\vec{\rho})\,e^{i\,\vec{\kappa}_T\vec{\rho}}. \tag{B23}$$

Eventually, the forward diffractive dissociation cross section of a quark reads

$$\left.\frac{d\sigma}{d(\ln\alpha)\,d^2q_T}\right|_{q_T=0} = \frac{1}{3}\int d^2\kappa_T\sum_s\,\mathrm{Tr}\,\hat{A}_s^{\dagger}(0,\vec{\kappa}_T,\alpha)\hat{A}_s(0,\vec{\kappa}_T,\alpha) = \frac{1}{(4\pi)^2}\int d^2\rho\left|\Psi_{qG}(\alpha,\vec{\rho})\,\frac{9}{8}\,\sigma_{qq}^{-}(\vec{\rho})\right|^2. \tag{B24}$$

We should emphasize that all above calculations are done for an arbitrary α.

2. Diffractive gluon radiation by a $\bar{q}q$ pair

Gluon radiation is an important contribution to the diffractive dissociation of a (virtual) photon,

$$\gamma^* N\to\bar{q}qGN. \tag{B25}$$

In analogy to the previous section we make use of the generalized unitarity relation,

$$\hat{A}_s(\gamma^*N\to\bar{q}qGN) = \frac{i}{2}\sum_f\left[\hat{A}_s(\bar{q}qGN\to\bar{q}qN_8^*)\,\hat{A}(\gamma^*N\to\bar{q}qN_8^*) + \sum_{s'}\hat{A}_{ss'}(\bar{q}qGN\to\bar{q}qGN_8^*)\,\hat{A}_{s'}(\gamma^*N\to\bar{q}qGN_8^*)\right], \tag{B26}$$

where the amplitudes are defined as follows:

$$\hat{A}(\gamma^* N \to \overline{q}qN_8^*) = [\tau_r \langle f|\hat{\gamma}_r(\vec{b}_1)|i\rangle + \overline{\tau}_r \langle f|\hat{\gamma}_r(\vec{b}_2)|i\rangle]\, \Psi^{-}_{qq}(\vec{\rho}_1 - \vec{\rho}_2, \alpha)\, |\overline{q}q\rangle_1; \tag{B27}$$

$$\hat{A}_{s'}(\gamma^* N \to \overline{q}qN_8^*) = \frac{i\sqrt{3}}{2} f_{s'rp}\{\tau_p[\langle f|\hat{\gamma}_r(\vec{b}_1)|i\rangle - \langle f|\hat{\gamma}_r(\vec{b}_3)|i\rangle]\, \Psi_{qG}(\vec{\rho}_1) + \overline{\tau}_p[\langle f|\hat{\gamma}_r(\vec{b}_2)|i\rangle - \langle f|\hat{\gamma}_r(\vec{b}_3)|i\rangle]\, \Psi_{qG}(\vec{\rho}_2)\}\, \Psi^{-}_{qq}(\vec{\rho}_1 - \vec{\rho}_2, \alpha)\, |\overline{q}q\rangle_1; \tag{B28}$$

$$\hat{A}_s(\overline{q}qGN \to \overline{q}qN_8^*) = -\frac{i\sqrt{3}}{2} f_{srp}\{\tau_p[\langle f|\hat{\gamma}_r(\vec{b}_1)|i\rangle - \langle f|\hat{\gamma}_r(\vec{b}_3)|i\rangle]\, \Psi_{qG}(\vec{\rho}_1) + \overline{\tau}_p[\langle f|\hat{\gamma}_r(\vec{b}_2)|i\rangle - \langle f|\hat{\gamma}_r(\vec{b}_3)|i\rangle]\, \Psi_{qG}(\vec{\rho}_2)\}; \tag{B29}$$

$$\hat{A}_{ss'}(\overline{q}qGN \to \overline{q}qGN_8^*) = \tau_r \langle f|\hat{\gamma}_r(\vec{b}_1)|i\rangle\, \delta_{ss'} + \overline{\tau}_r \langle f|\hat{\gamma}_r(\vec{b}_2)|i\rangle\, \delta_{ss'} + i\, f_{ss'r} \langle f|\hat{\gamma}_r(\vec{b}_3)|i\rangle. \tag{B30}$$

Here $\vec{b}_1 = \vec{b} + \vec{r}_1$, $\vec{b}_2 = \vec{b} + \vec{r}_2$, $\vec{b}_3 = \vec{b} + \vec{\rho}$ are the impact parameters of the quark, antiquark and gluon, respectively; $\vec{b}$ is the photon impact parameter; $\vec{\rho}_{1,2} = \vec{\rho} - \vec{r}_{1,2}$; Ψ^{-}_{qq} and $|\overline{q}q\rangle$ are spatial and color parts of the $\overline{q}q$-component of the photon wave function, respectively. The matrices $\tau_r = \lambda_r/2$ and $\overline{\tau}_r = \lambda_r^*/2$ act on the color indices of quark and antiquark respectively. The indices s, s' mark the color states of the gluons in intermediate and final states.

Note that the condition of color neutrality of the singlet state $|\overline{q}q\rangle$ leads to the relation

$$(\tau_r + \overline{\tau}_r)\, |\overline{q}q\rangle = 0. \tag{B31}$$

Substitution of Eqs. (B26)–(B30) into Eq. (B25) leads to the following expression for the amplitude of diffractive dissociation of the photon:

$$\begin{aligned}\hat{A}(\gamma^* N \to \overline{q}qGN) = \frac{i3\sqrt{3}}{16}\{&(i\, f_{srp}[\tau_p\, \tau_r + \tau_r\, \tau_p][s(\vec{b}_1, \vec{b}_1) - s(\vec{b}_3, \vec{b}_1)] + i\, f_{srp}[\tau_p\, \overline{\tau}_r + \overline{\tau}_r\, \tau_p] \\ &\times [s(\vec{b}_1, \vec{b}_2) - s(\vec{b}_3, \vec{b}_2)] + f_{ss'r}\, f_{s'rp}\, \tau_p[s(\vec{b}_3, \vec{b}_1) - s(\vec{b}_3, \vec{b}_3)])\, \Psi_{qG}(\vec{\rho}_1) + (i\, f_{srp}[\overline{\tau}_p\, \overline{\tau}_r + \overline{\tau}_r\, \overline{\tau}_p] \\ &\times [s(\vec{b}_2, \vec{b}_2) - s(\vec{b}_2, \vec{b}_3)] + i\, f_{srp}[\overline{\tau}_p\, \tau_r + \tau_r\, \overline{\tau}_p][s(\vec{b}_2, \vec{b}_1) - s(\vec{b}_3, \vec{b}_1)] + f_{ss'r}\, f_{s'rp}\, \overline{\tau}_p \\ &\times [s(\vec{b}_3, \vec{b}_2) - s(\vec{b}_3, \vec{b}_3)])\, \Psi_{qG}(\vec{\rho}_2)\}\, |\overline{q}q\rangle_1\, \Psi^{-}_{qq}(\vec{\rho}_1 - \vec{\rho}_2, \alpha),\end{aligned} \tag{B32}$$

where we made use of the completeness condition, $\Sigma_f |f\rangle\langle f| = 1$ (see Appendix B 1).

In order to simplify Eq. (B32) we apply a few relations as follows. Since $f_{srp} = -f_{spr}$ we find

$$f_{srp}[\tau_p \tau_r + \tau_r \tau_p] = f_{srp}[\overline{\tau}_p \overline{\tau}_r + \overline{\tau}_r \overline{\tau}_p] = 0. \tag{B33}$$

Then, relying on the condition (B31) we find

$$(\tau_p \overline{\tau}_r + \overline{\tau}_r \tau_p)\, |\overline{q}q\rangle_1 = 2\, \tau_p \overline{\tau}_r\, |\overline{q}q\rangle_1 = -2\, \tau_p \tau_r\, |\overline{q}q\rangle_1; \tag{B34}$$

$$(\overline{\tau}_p\, \tau_r + \tau_r\, \overline{\tau}_p)\, |\overline{q}q\rangle_1 = 2\, \overline{\tau}_p\, \tau_r\, |\overline{q}q\rangle_1 = -2\, \overline{\tau}_p\, \overline{\tau}_r\, |\overline{q}q\rangle_1. \tag{B35}$$

We also use the relations

$$i\, f_{srp} \tau_p \tau_r = \frac{3}{2}\tau_s; \quad i\, f_{srp} \overline{\tau}_p \overline{\tau}_r = \frac{3}{2}\overline{\tau}_s; \quad f_{ss'r}\, f_{s'rp} = 3\, \delta_{sp}, \tag{B36}$$

and the symmetry condition, $s(\vec{b}_k, \vec{b}_l) = s(\vec{b}_l, \vec{b}_k)$, and eventually arrive at a modified form of Eq. (B32)

$$\hat{A}_s(\gamma^* N \to \overline{q}qGN) = \frac{9\sqrt{3}}{16}[\tau_s \Psi_{qG}(\vec{\rho}_1) + \overline{\tau}_s\, \Psi_{qG}(\vec{\rho}_2)]\, |\overline{q}q\rangle_1 \Psi^{-}_{qq}(\vec{\rho}_1 - \vec{\rho}_2, \alpha)[s(\vec{b}_2, \vec{b}_3) + s(\vec{b}_1, \vec{b}_3) - s(\vec{b}_1, \vec{b}_2) - s(\vec{b}_3, \vec{b}_3)]. \tag{B37}$$

The last factor in square brackets can be represented as

$$P(\vec{b}_1,\vec{b}_2;\vec{b}_3)\equiv s(\vec{b}_2,\vec{b}_3)+s(\vec{b}_1,\vec{b}_3)-s(\vec{b}_1,\vec{b}_2)-s(\vec{b}_3,\vec{b}_3)$$

$$\equiv\frac{1}{2}\{[s(\vec{b}_1,\vec{b}_1)+s(\vec{b}_2,\vec{b}_2)-2s(\vec{b}_1,\vec{b}_2)]-[s(\vec{b}_2,\vec{b}_2)+s(\vec{b}_3,\vec{b}_3)-2s(\vec{b}_2,\vec{b}_3)]$$

$$-[s(\vec{b}_1,\vec{b}_1)+s(\vec{b}_3,\vec{b}_3)-2s(\vec{b}_1,\vec{b}_3)]\}. \tag{B38}$$

Then, the forward diffraction amplitude ($q_T=0$) in impact parameter representation has the form

$$\frac{1}{2\pi}\int d^2b\,\hat{A}_s(\vec{b},\vec{\rho}_1\vec{\rho}_2)=-\frac{i}{4\pi}\Sigma(\vec{\rho}_1,\vec{\rho}_2)\left[\frac{\sqrt{3}}{2}\tau_s\,\Psi_{qG}(\vec{\rho}_1)+\frac{\sqrt{3}}{2}\overline{\tau_s}\,\Psi_{qG}(\vec{\rho}_2)\right]|\overline{qq}\rangle_1\,\Psi_{\overline{qq}}(\vec{\rho}_1-\vec{\rho}_2,\alpha), \tag{B39}$$

where $\Sigma(\vec{\rho}_1,\vec{\rho}_2)$ is introduced in Eq. (73).

From Eq. (B39) one easily gets the forward diffractive cross section

$$\left.\frac{d\sigma(\gamma^*N\to\overline{q}qGN)}{d(\ln\alpha_G)\,dq_T}\right|_{\substack{q_T=0\\ \alpha_G\to 0}}=\frac{1}{(4\pi)^2}\int d^2\rho_1\,d^2\rho_2\,d\alpha\,|\Psi_{\overline{qq}}(\vec{\rho}_1-\vec{\rho}_2,\alpha)[\Psi_{qG}(\vec{\rho}_1)-\Psi_{qG}(\vec{\rho}_2)]\,\Sigma(\vec{\rho}_1,\vec{\rho}_2)|^2. \tag{B40}$$

3. Diffractive photon radiation, $qN\to\gamma qN$

Diffractive electromagnetic radiation is calculated in analogy to what was done in Appendix B 1 for gluon radiation. Since the photon does not interact with the gluonic field of the target the structure of all the amplitudes in the relation

$$\hat{A}(qN\to q\gamma N)=\frac{i}{2}\sum_f\,[\hat{A}^\dagger(q\gamma N\to qN_8^*)\,\hat{A}(qN\to qN_8^*)+\hat{A}^\dagger(q\gamma N\to q\gamma N_8^*)\,\hat{A}(qN\to q\gamma N_8^*)], \tag{B41}$$

turns out to be much simpler:

$$\hat{A}(qN\to qN_8^*)=\tau_r\langle f|\hat{\gamma}_r(\vec{b}_1)|i\rangle; \tag{B42}$$

$$\hat{A}(q\gamma N\to q\gamma N_8^*)=\tau_r\langle f|\hat{\gamma}_r(\vec{b}_2)|i\rangle; \tag{B43}$$

$$\hat{A}(qN\to q\gamma N_8^*)=\hat{A}(q\gamma N\to q\gamma N_8^*)=\tau_r[\langle f|\hat{\gamma}_r(\vec{b}_1)|i\rangle-\langle f|\hat{\gamma}_r(\vec{b}_2)|i\rangle]\,\Psi_{q\gamma}(\vec{\rho},\alpha). \tag{B44}$$

Here $\vec{b}_1=\vec{b}$, $\vec{b}_2=\vec{b}-\alpha\,\vec{\rho}$ are the impact parameters of the quark before and after radiation of the photon; $\vec{\rho}$ is the transverse separation between the quark and photon in the final state; and α is the fraction of the quark light cone momentum carried away by the photon. $\Psi_{q\gamma}(\vec{\rho},\alpha)$ is the distribution function for the $q\gamma$ fluctuation of the quark. The initial, $|i\rangle$, and final, $|f\rangle$, states of the target, as well as the operators $\hat{\gamma}(\vec{b}_k)$ ($k=1,2$) are the same as in Appendix B 1.

After substitution of Eqs. (B42)–(B44) into Eq. (B41) we get

$$\hat{A}(qN\to q\gamma N)=\frac{i}{2}\{\tau_r\,\tau_{r'}\,[\Phi_{rr'}(\vec{b}_1,\vec{b}_1)-\Phi_{rr'}(\vec{b}_1,\vec{b}_2)+\Phi_{rr'}(\vec{b}_2,\vec{b}_1)-\Phi_{rr'}(\vec{b}_2,\vec{b}_2)]\}. \tag{B45}$$

Here the functions $\Phi_{rr'}(\vec{b}_k,\vec{b}_l)$ are defined in Appendix B 1. Then, the amplitude in impact parameter representation reads

$$\hat{A}(\vec{b},\vec{\rho})=\frac{i}{2}[s(\vec{b}_1,\vec{b}_1)-s(\vec{b}_2,\vec{b}_2)]=\frac{i}{2}[s(\vec{b},\vec{b})-s(\vec{b}-\alpha\,\vec{\rho},\vec{b}-\alpha\,\vec{\rho})]. \tag{B46}$$

After Fourier transform to the momentum representation we get for the forward diffractive amplitude of photon radiation,

$$A(\vec{q}_T,\vec{\kappa}_T)|_{q_T=0}=\frac{1}{(2\pi)^2}\int d^2b\,d^2\rho\,\exp(i\,\vec{q}_T\,\vec{b}+i\,\vec{\kappa}_T\,\vec{\rho})\,\hat{A}(\vec{b}_T,\vec{\rho}_T)\Big|_{q_T=0}=0. \tag{B47}$$

Thus, the direct calculation of Feynman diagrams confirms our previous conclusion (Appendix A 4) that a quark does not diffractively emit electromagnetic radiation if the momentum transfer with the target is zero (as different from the statement in [20]). A hadron, however, can radiate in forward scattering.

APPENDIX C: THE TRIPLE-POMERON COUPLING

In the limit of vanishing quark and gluon masses the quark-gluon wave function (56) retains only the second term $\propto\vec{\Phi}_1$ which has the form (27). Bilinear combinations of this wave function averaged over final polarizations can be represented as follows:

$$|\Phi_1(\vec{\rho}_i,\alpha)|^2=\frac{1}{(2\pi)^2}\int_{b(\alpha)^2}^{\infty}dt\,e^{-t\rho_i^2}, \tag{C1}$$

$$\vec{\Phi}_1(\vec{\rho}_i,\alpha)\cdot\vec{\Psi}_1(\vec{\rho}_k)=\frac{\vec{\rho}_i\cdot\vec{\rho}_k}{(2\pi)^2}\int_{b^2(\alpha)/2}^{\infty}du\int_{b^2(\alpha)/2}^{\infty}dt\,e^{-t\rho_i^2-u\rho_i^2}. \tag{C2}$$

This together with Eqs. (30) and (79) allows to integrate analytically over the coordinates of the quarks and the gluon in Eq. (78). Finally integrating over t and u we arrive at

$$G_{3P}(NN\to XN)=\frac{\alpha_s}{(4\pi)^2}\left(\frac{9}{8}\sigma_0\right)^2[F_1(x,z)-F_2(x,z)], \tag{C3}$$

where $x=b^2(0)\rho_0^2$, $z=z_N=2\langle r^2\rangle_p/\rho_0^2$, and

$$F_1(x,z)=\ln\left[\frac{(x+1)^2}{x(x+2)}\right]+2s_1\ln\left[\frac{(x+1)(x+s_1)}{x(1+x+s_1)}\right]+\frac{2}{3}s_2\left[2\ln\left(\frac{s_1x+s_2}{xs_1}\right)-\ln\left(\frac{x+2s_2}{x}\right)\right]$$
$$+\frac{1}{3}s_3s_4\left[2\ln\left(\frac{s_1x+s_3s_4}{xs_1}\right)-\ln\left(\frac{x+2s_4}{x}\right)\right]. \tag{C4}$$

Here

$$s_1=\frac{1}{1+z},\quad s_2=\frac{1}{1+2z},\quad s_3=\frac{2}{2+z},\quad s_4=\frac{2}{2+3z},\quad s_5=\frac{4}{4+3z}; \tag{C5}$$

$$zF_2(x,z)=\sum_{i=1}^{14}\frac{g(i)}{\beta(i)}\ln\left[\frac{\delta(i)\,\gamma(i)}{\delta(i)\,\gamma(i)-\beta^2(i)}\right], \tag{C6}$$

where

$i=1$ $g=2/3$, $\beta=1/z+2$, $\gamma=\delta=x/2+\beta$;

$i=2$ $g=2$, $\beta=1/z+1$, $\gamma=\delta=x/2+\beta$;

$i=3$ $g=-10/3$, $\beta=1/z+1$, $\delta=x/2+\beta$, $\gamma=\delta+1$;

$i=4$ $g=1$, $\beta=1/z$, $\gamma=\delta=x/2+\beta$;

$i=5$ $g=-4$, $\beta=1/z$, $\delta=x/2+\beta$, $\gamma=\delta+1$;

$i=6$ $g=5/3$, $\beta=1/z+2$, $\gamma=\delta=x/2+\beta+1$;

$i=7$ $g=2$, $\beta=1/z$, $\delta=x/2+\beta$, $\gamma=\delta+2$;

$i=8$ $g=s_4/3$, $\beta=1/z+1/2$, $\gamma=\delta=x/2+\beta$;

$i=9$ $g=-2s_5/3$, $\beta=1/z+s_5/4$, $\delta=x/2+\beta$, $\gamma=\delta+1$;

$i=10$ $g=2s_5/3$, $\beta=1/z+1+s_5/4$, $\gamma=\delta=x/2+\beta$;

$i=11$ $g=-s_4/3$, $\beta=1/z-s_4/2$ $\gamma=\delta=x/2+\beta+s_4$;

$i=12$ $g=-2s_5/3$, $\beta=1/z+1-s_5/4$, $\gamma=\delta=x/2+\beta+s_5/2$;

$$i=13 \quad g=-2s_5/3, \quad \beta=1/z-s_5/4, \quad \delta=x/2+\beta+s_5/2, \quad \gamma=\delta+1;$$

$$i=14 \quad g=2s_4/3, \quad \beta=1/z, \quad \delta=x/2+\beta+1/2, \quad \gamma=x/2+\beta+s_4/2. \tag{C7}$$

The effective triple-Pomeron coupling $G_{3P}(MN\to XN)$ for diffractive dissociation of a meson M can be calculated in a similar way assuming a Gaussian shape of the quark wave function of the meson

$$|\Psi_{M\to\bar{q}q}(\vec{r})|^2=\frac{1}{\pi R^2}e^{-r^2/R^2}, \tag{C8}$$

where $R^2=8\langle r_M^2\rangle_{ch}/3$. The triple-Pomeron coupling is smaller by a factor 2/3 (different number of valence quarks) and has a form similar to Eq. (C3),

$$G_{3P}(MN\to XN)=\frac{2\,\alpha_s}{3\,(4\pi)^2}\left(\frac{9}{8}\sigma_0\right)^2[F_1^M(x,z_M)-F_2^M(x,z_M)], \tag{C9}$$

but $z_M=R^2/\rho_0^2\neq z_N$ and the functions $F_{1,2}^M$ are different too. The expression for $F_1^M(x,z_M)$ results from $F_1(x,z)$ via the replacement $s_3\to 1$, $s_4\to s_2$ and $z\to z_M$.

The expression for $F_2(x,z_M)$ follows from $F_2(x,z)$ after moderate modifications in Eq. (C7): $g(1)=1$, $g(3)=-4$, $g(6)=2$, all $g(i)=0$ for $i\geqslant 8$ and $z\to z_M$.

In the case of diffractive dissociation of a photon, the calculations are more complicated since the spatial distribution of quarks in the photon is very different from a Gaussian. Nevertheless, it can be represented as a superposition of Gaussians,

$$|\Psi_{\gamma\to\bar{q}q}(\vec{r},\alpha)|^2=\frac{\alpha_{em}N_c\sum Z_q^2}{2\,\pi}\int_0^{1/a^2(\alpha)}\frac{dR^2}{R^2}\left(\frac{1}{\pi R^2}e^{-r^2/R^2}\right). \tag{C10}$$

Then, the effective coupling $G_{3P}(\gamma N\to XN)$ takes a form similar to Eqs. (C3) and (C9),

$$G_{3P}(\gamma N\to XN)=\frac{2\alpha_{em}\alpha_s N_c\sum Z_q^2}{6\,(2\pi)^3}\left(\frac{9}{8}\sigma_0\right)^2[F_1^\gamma(x,z_\gamma)-F_2^\gamma(x,z_\gamma)], \tag{C11}$$

where $z_\gamma=[a^2(\alpha)\,\rho_0^2]^{-1}$ and

$$F_{1,2}^\gamma(x,z_\gamma)=\int_0^{z_\gamma}\frac{dv}{v}F_{1,2}^M(x,v). \tag{C12}$$

[1] J.B. Kogut and D.E. Soper, Phys. Rev. D **1**, 2901 (1970).
[2] J.M. Bjorken, J.B. Kogut, and D.E. Soper, Phys. Rev. D **3**, 1382 (1971).
[3] N.N. Nikolaev and B.G. Zakharov, Z. Phys. C **49**, 607 (1991).
[4] E.M. Levin, A.D. Martin, M.G. Ryskin, and T. Teubner, Z. Phys. C **74**, 671 (1997).
[5] A.B. Zamolodchikov, B.Z. Kopeliovich, and L.I. Lapidus, Pis'ma Zh. Éksp. Teor. Fiz. **33**, 612 (1981) [JETP Lett. **33**, 595 (1981)].
[6] A.H. Mueller, Nucl. Phys. **B415**, 373 (1994); A.H. Mueller and B. Patel, *ibid.* **B425**, 473 (1994).
[7] B.Z. Kopeliovich and B.G. Zakharov, Phys. Rev. D **44**, 3466 (1991).
[8] J. Hüfner and B. Povh, Phys. Rev. D **46**, 990 (1992).
[9] L.L. Frankfurt, W. Koepf, and M. Strikman, Phys. Rev. D **54**, 3194 (1996).
[10] K. Golec-Biernat and M. Wüsthoff, Phys. Rev. D **59**, 014017 (1999); **60**, 114023 (1999).
[11] J.R. Forshaw, G. Kerley, and G. Shaw, Phys. Rev. D **60**, 074012 (1999).
[12] B.Z. Kopeliovich, J. Raufeisen, and A.V. Tarasov, Phys. Lett. B **440**, 151 (1998).
[13] J. Raufeisen, A.V. Tarasov, and O. Voskresenskaya, Eur. Phys. J. A **5**, 173 (1999).
[14] B.G. Zakharov, Yad. Fiz. **61**, 924 (1998) [Phys. At. Nucl. **61**, 838 (1998)].
[15] V.M. Braun, P. Górnicki, L. Mankiewicz, and A. Schäfer, Phys. Lett. B **302**, 291 (1993).
[16] M. D'Elia, A. Di Giacomo, and E. Meggiolaro, Phys. Lett. B **408**, 315 (1997).
[17] T. Schäfer and E.V. Shuryak, Rev. Mod. Phys. **70**, 323 (1998).
[18] N.N. Nikolaev and B.G. Zakharov, Z. Phys. C **64**, 631 (1994); M. Genovese, N.N. Nikolaev, and B.G. Zakharov, Zh. Éksp. Teor. Fiz. **108**, 1155 (1995) [JETP **81**, 633 (1995)].

[19] J. Bartels, H. Jung, and M. Wüsthoff, Eur. Phys. J. C **11**, 111 (1999).
[20] B.Z. Kopeliovich, Phys. Lett. B **447**, 308 (1999).
[21] L.V. Gribov, E.M. Levin, and M.G. Ryskin, Nucl. Phys. **B188**, 555 (1981); Phys. Rep. **100**, 1 (1983).
[22] E.M. Levin and M.G. Ryskin, Yad. Fiz. **41**, 472 (1985) [Sov. J. Nucl. Phys. **41**, 300 (1985)].
[23] L.L. Frankfurt, S. Liuti, and M.I. Strikman, Phys. Rev. Lett. **65**, 1725 (1990).
[24] L. McLerran and R. Venugopalan, Phys. Rev. D **49**, 2233 (1994); **49**, 3352 (1994); **50**, 2225 (1994).
[25] A.H. Mueller, Nucl. Phys. **B558**, 285 (1999).
[26] A.L. Ayala, M.B. Gay Ducati, and E.M. Levin, Nucl. Phys. **B493**, 305 (1997).
[27] K.J. Eskola, J. Qiu, and X.-N. Wang, Phys. Rev. Lett. **72**, 36 (1994).
[28] K.J. Eskola, V.J. Kolhinen, and P.V. Ruuskanen, Nucl. Phys. **B535**, 351 (1998).
[29] S. Kumano and K. Umekawa, hep-ph/9803359.
[30] L.L. Frankfurt and M.I. Strikman, Eur. Phys. J. A **5**, 293 (1999).
[31] L. Alvero, L.L. Frankfurt, and M.I. Strikman, Eur. Phys. J. A **5**, 97 (1999).
[32] G. Piller and W. Weise, Phys. Rep. **330**, 1 (2000).
[33] V.N. Gribov, Zh. Éksp. Teor. Fiz. **56**, 892 (1969) [Sov. Phys. JETP **29**, 483 (1969)]; **57**, 1306 (1969) [**30**, 709 (1970)].
[34] L. Alvero, J.C. Collins, and J.J. Whitmore, Phys. Rev. D **59**, 074022 (1999).
[35] L. Alvero, J.C. Collins, and J.J. Whitmore, ''Tests of Factorization in Diffractive Charm Production and Double Pomeron Exchange,'' hep-ph/9806340.
[36] B.Z. Kopeliovich, A. Schäfer, and A.V. Tarasov, Phys. Rev. C **59**, 1609 (1999).
[37] I. Halperin and A. Zhitnitsky, Phys. Rev. D **56**, 184 (1997).
[38] R.P. Feynman and A.R. Gibbs, *Quantum Mechanics and Path Integrals* (McGraw-Hill, New York, 1965).
[39] F.E. Low, Phys. Rev. D **12**, 163 (1975).
[40] S. Nussinov, Phys. Rev. Lett. **34**, 1286 (1975).
[41] B.Z. Kopeliovich and B. Povh, Mod. Phys. Lett. A **13**, 3033 (1998).
[42] S. Amendolia *et al.*, Nucl. Phys. **B277**, 186 (1986).
[43] Particle Data Group, R.M. Barnett *et al.*, Phys. Rev. D **54**, 1 (1996), p. 191.
[44] H1 Collaboration, S. Aid *et al.*, Z. Phys. C **69**, 27 (1995).
[45] ZEUS Collaboration, M. Derrick *et al.*, Phys. Lett. B **293**, 465 (1992).
[46] Yu.M. Kazarinov, B.Z. Kopeliovich, L.I. Lapidus, and I.K. Potashnikova, Zh. Éksp. Teor. Fiz. **70**, 1152 (1976) [Sov. Phys. JETP **43**, 598 (1976)].
[47] J. Hüfner, B.Z. Kopeliovich, and J. Nemchik, Phys. Lett. B **383**, 362 (1996).
[48] HERMES Collaboration, K. Ackerstaff *et al.*, Phys. Rev. Lett. **82**, 3025 (1999).
[49] G.R. Brookes *et al.*, Phys. Rev. D **8**, 2826 (1973); E.A. Arakelian *et al.*, Phys. Lett. **79B**, 143 (1978).
[50] Y. V. Kovchegov and A.H. Mueller, Nucl. Phys. **B529**, 451 (1998).
[51] U.A. Wiedemann and M. Gyulassy, Nucl. Phys. **B560**, 345 (1999).
[52] B.Z. Kopeliovich, *Soft Component of Hard Reactions and Nuclear Shadowing (DIS, Drell-Yan reaction, heavy quark production)*, Proceedings of the Workshop Hirschegg'95: Dynamical Properties of Hadrons in Nuclear Matter, Hirschegg, 1995, edited by H. Feldmeier and W. Nörenberg (Darmstadt, 1995), p. 102 (hep-ph/9609385).
[53] S.J. Brodsky, A. Hebecker, and E. Quack, Phys. Rev. D **55**, 2584 (1997).
[54] V. Novikov, M. Shifman, A. Veinshtein, and V. Zakharov, Nucl. Phys. **B191**, 301 (1981).
[55] A. Casher, H. Neubereger, and S. Nussinov, Phys. Rev. D **20**, 179 (1979).
[56] B. Blättel *et al.*, Phys. Rev. Lett. **70**, 896 (1993).
[57] V. Barone *et al.*, Z. Phys. C **58**, 541 (1993).
[58] R.E. Cutkosky, J. Math. Phys. **1**, 429 (1960).
[59] CDF Collaboration, F. Abe *et al.*, Phys. Rev. D **50**, 5535 (1994).
[60] E. Gotsman, E. Levin, and U. Maor, Phys. Lett. B **438**, 229 (1998).
[61] K. Goulianos and J. Montanha, Phys. Rev. D **59**, 114017 (1999).
[62] T. Udem *et al.*, Phys. Rev. Lett. **79**, 2646 (1997).
[63] T. Chapin *et al.*, Phys. Rev. D **31**, 17 (1985).
[64] H1 Collaboration, C. Adloff *et al.*, Z. Phys. C **74**, 221 (1997).
[65] S. Erhan and P.E. Schlein, Phys. Lett. B **427**, 389 (1998).
[66] O.V. Kancheli, Zh. Éksp. Teor. Fiz., Pis'ma Red. **18**, 465 (1973) [JETP Lett. **18**, 274 (1973)].
[67] A.H. Mueller and J.W. Qiu, Nucl. Phys. **B268**, 427 (1986).
[68] N. Hammon, H. Stöcker, and W. Greiner, Phys. Lett. B **448**, 290 (1999).
[69] V. Karmanov and L.A. Kondratyuk, Zh. Éksp. Teor. Fiz., Pis'ma Red. **18**, 451 (1973) [JETP Lett. **18**, 266 (1973)].
[70] P.V.R. Murthy *et al.*, Nucl. Phys. **B92**, 269 (1975).
[71] H1 Collaboration, contribution pa02-060 to ICHEP96, Warshaw, 1996.
[72] ZEUS Collaboration, contribution N-643 to EPS97, Jerusalem, 1997.
[73] R.J. Glauber, Phys. Rev. **100**, 242 (1955); *Lectures in Theoretical Physics*, edited by W.E. Britting and D.G. Dunham (Interscience, New York, 1959), Vol. 1, p. 315.
[74] B.Z. Kopeliovich and L.I. Lapidus, Pis'ma Zh. Éksp. Teor. Fiz. **28**, 664 (1978) [JETP Lett. **28**, 614 (1978)].
[75] B.Z. Kopeliovich, J. Raufeisen, and A.V. Tarasov (in preparation).
[76] B.Z. Kopeliovich, J. Raufeisen, and A.V. Tarasov, hep-ph/0003136.
[77] B.Z. Kopeliovich and J. Nemchik, Phys. Lett. B **368**, 187 (1996).
[78] J. Hüfner and B.Z. Kopeliovich, Phys. Lett. B **445**, 223 (1998).
[79] J. Huefner, Y.B. He, and B.Z. Kopeliovich, Eur. Phys. J. A **7**, 239 (2000).
[80] A.H. Mueller, Nucl. Phys. **B572**, 227 (2000).
[81] E. Feinberg and I.Ya. Pomeranchuk, Nuovo Cimento Suppl. **3**, 652 (1956).
[82] M.L. Good and W.D. Walker, Phys. Rev. **120**, 1857 (1960).
[83] H.I. Miettinen and J. Pumplin, Phys. Rev. D **18**, 1696 (1978).